

PEOPLE'S DEMOCRATIC REPUBLIC OF ALGERIA
MINISTRY OF HIGHER EDUCATION AND SCIENTIFIC RESEARCH
ZIANE ACHOUR UNIVERSITY OF DJELFA
FACULTY OF SCIENCE AND TECHNOLOGY



Laboratoire Modélisation Simulation et Optimisation des Systèmes Complexes
Réels (MSOSCR)

DOCTORAL THESIS (DLMD)
FACULTY: APPLIED AUTOMATIC
SPECIALTY: MODELING OF INFORMATIONAL SIGNALS
BY: CHINOUN AHMED
WITH TITLE:
GENERALIZED LATTICE STRUCTURE STUDY OF MULTIDIMENSIONAL
FIR FILTERS

PUBLICLY DEFENDED ON: DECEMBER 26, 2020
BEFORE THE JURY COMPOSED OF:

PRESIDENT: OMAR MANSOUR (PR., UNIVERSITY OF DJELFA)

SUPERVISOR: LAHCÈNE MITICHE (PR., UNIVERSITY OF DJELFA)

**EXAMINER: AMEL BAHA HOUDA ADAMOU-MITICHE (PR.,
UNIVERSITY OF DJELFA)**

EXAMINER: MAAMAR AHFIR (PR., UNIVERSITY OF MEDEA)

EXAMINER: HAKIM AZIZI (MCA, UNIVERSITY OF DJELFA)

الشعبية الجزائرية الديمقراطية الجمهورية
REPUBLIC ALGERIENNE DEMOCRATIQUE ET POPULAIRE
MINISTERE DE L'ENSEIGNEMENT SUPERIEUR ET DE LA RECHERCHE SCIENTIFIQUE
UNIVERSITE ZIANE ACHOUR DE DJELFA



FACULTE DES SCIENCES ET TECHNOLOGIE
LABORATOIRE MODELISATION SIMULATION ET OPTIMISATION DES SYSTEMES COMPLEXES REELS

THESE DE DOCTORAT (DLMD)
FILIERE : AUTOMATIQUE APPLIQUEE
SPECIALITE : MODELISATION DES SIGNAUX INFORMATIONNELS
PAR : CHINOUN AHMED
INTITULEE :
ETUDE DE STRUCTURE EN TREILLIS GENERALISE DES FILTRES RIF
MULTIDIMENSIONNELS

SOUTENUE PUBLIQUEMENT LE : 26 DECEMBRE 2020
DEVANT LE JURY COMPOSE DE :

PRESIDENT : OMAR MANSOUR (PR., UNIVERSITE DE DJELFA)

DIRECTEUR DE THESE : LAHCENE MITICHE (PR., UNIVERSITE DE DJELFA)

EXAMINATEUR : AMEL BAHA HOUDA ADAMOU-MITICHE (PR., UNIVERSITE DE DJELFA)

EXAMINATEUR : MAAMAR AHFIR (PR., UNIVERSITE DE MEDEA)

EXAMINATEUR : HAKIM AZIZI (MCA, UNIVERSITE DE DJELFA)

I would like to dedicate this thesis to my loving parents, my family members
and to everyone who knows me.

Acknowledgements

I am fortunate to have this opportunity to thank the many people who have helped in the preparation of this thesis. First of all I am most indebted to my advisor, professor Lahcène Mitiche, for his guidance and motivation. Also, I wish to express my sincere gratitude to professor A. B. H Adamou-Mitiche for her convivial support and comments on many subject matters closely related to the preparation of this thesis for being a constant source of ideas. I wish to acknowledge the patience and assistance of my wife. She has been a continuous source of inspiration. We wish to thank science and technology Department of Djelfa University and all the administrators, teachers, and special thanks to the members of examining board.

Abstract

The aim of the minimal state space realization problem is to find a state space model of minimal size of the given system. The main subject of this thesis is in the crucial problem of constructing state-space realizations of 2-D/3-D linear systems from proposed structures in lattice and ladder lattice form. We use this proposed structures on lattice and ladder lattice to design 2-D digital notch filter and 3-D digital notch filter.

الهدف من مشكلة تحقيق الحد الأدنى من فضاء الحالة هو العثور على نموذج من فضاء الحالة ذا حد أدنى من نظام معطي. يتمثل الموضوع الرئيسي لهذه الدراسة في المشكلة المتمثلة في إنشاء الحد الأدنى من تحقيق فضاء الحالة لنظام خطي ثنائي الأبعاد و ثلاثي الأبعاد من هياكل مقترحة في شكل شبكات شبكات سلم. نستخدم هذه الهياكل المقترحة على الشبكة الشبكة الشبكية للسلم لتصميم مرشح الشق الرقمي ثنائي الأبعاد ومرشح الشق الرقمي ثلاثي الأبعاد.

Le problème de la minimalité de l'espace d'état est de trouver un modèle d'espace d'état de taille minimale d'un système donné. Le sujet principal de cette thèse est de résoudre le problème crucial de la construction d'une réalisations d'état minimal d'un système linéaire 2-D / 3-D à partir de structures proposées sous forme de treillis et de treillis en échelle. Nous utilisons ces structures proposées en treillis et en treillis en échelle pour concevoir un filtre numérique coupe-bande 2-D et un filtre numérique coupe-bande 3-D.

Table of contents

List of figures	xiii
Introduction	1
1 Multi-dimensional signals and systems	5
1.1 Introduction	5
1.2 Multi-dimensional signals	5
1.2.1 Kronecker delta function	6
1.2.2 The Heaviside step function	7
1.2.3 Separable sequence	8
1.2.4 Linearity	9
1.2.5 Shift invariance	9
1.3 Multidimensional systems	10
1.4 Fundamental operations on Multidimensional system	10
1.4.1 Linear system	10
1.4.2 Shift invariant systems	11
1.4.3 Convolution	11
1.4.4 Properties of N-D convolution	12
1.5 N-D z-transform	12
1.5.1 Properties of N-D z-transform	13
1.5.2 Inverse Z-Transform	14
1.6 N-D Fourier transform	15
1.7 Stability	15
1.7.1 BIBO stability	15
1.7.2 Necessary and sufficient conditions stability in N-Dimensions	16
1.7.3 Method to derive necessary and sufficient stability con- ditions	16
1.8 State-space models and transfer function	17

1.8.1	Givone–Roesse’s model	17
1.8.2	Recursive equation	18
1.8.3	Transfer function	18
1.8.4	Differences between transfer functions and state-space models	19
1.9	N-Dimensional digital filter	19
1.10	Realization of digital filters	20
1.10.1	Direct form I	20
1.10.2	Direct form II	21
1.10.3	Cascade Realization	21
1.10.4	Parallel Realization	22
1.10.5	Lattice and ladder realisation	22
1.11	Conclusion	23
2	Minimal state-space realization in linear systems	25
2.1	Introduction	25
2.2	The minimal state-space realization problem for LTI systems .	26
2.3	Linear time-invariant systems	27
2.4	Minimal realization based on reduction of nonminimal realizations	28
2.5	Minimal realization of impulse responses	28
2.6	The minimal partial realization problem	28
2.7	Minimal realization based on step response data	28
2.8	Rational approximation	29
2.9	Model reduction	30
2.10	Identification	31
2.11	Positive linear systems	31
2.12	Max-plus-algebraic models	32
2.13	Linear time-varying models	33
2.14	Nonlinear models	33
2.15	Multi-dimensional minimal state-space realization	33
2.16	Conclusion	37
3	Minimal state-space realizations of proposed structures in lattice and ladder-lattice form	39
3.1	Introduction	39
3.2	Proposed lattice structure and realization	40

3.2.1	Proposed ladder lattice 2-d digital filter	40
3.2.2	Realization	41
3.2.3	State space realization	43
3.2.4	Example	44
3.3	Interpretation	46
3.4	Proposed 3-D Lattice Structure	47
3.4.1	Proposed FIR Lattice Structure	47
3.4.2	Proposed Recursive Lattice Structure	48
3.4.3	State Space Realization	49
3.4.4	Interpretation	51
4	Application of the proposed realization two and Three-Dimensional IIR Notch Filter Design:simulation and interpretation	53
4.1	Introduction	53
4.2	Notch filter characteristics	54
4.3	Applications of notch filters	54
4.4	Digital notch filter design techniques	56
4.5	Notch filter based on all-pass filter	57
4.6	Two-Dimensional IIR Notch Filter Design	58
4.6.1	Proposed lattice ladder structure	59
4.6.2	Two-Dimensional IIR Notch Filter Design	60
4.6.3	Design Two-Dimensional IIR Notch Filter using an all-pole filter	60
4.6.4	Parallel of Two-Dimensional IIR Notch Filter	62
4.6.5	simulation examples	63
4.6.6	2-D IIR notch filter design	65
4.6.7	Removing interference of an image	66
4.6.8	Interpretation	67
4.7	3-D IIR Notch Filter Design	68
4.7.1	3-D IIR All-pass Filter Design	68
4.7.2	3-D IIR filter design	69
4.7.3	3-D IIR spatial straight line filter design	70
4.7.4	Implementation and design 3-D IIR Notch filter	72
5	Conclusions	77
	References	79

Appendix A	85
Appendix B	87
Appendix C	89
C.0.1 problem statement	89
C.0.2 State-space realization	90
Appendix D	95

List of figures

1.1	2-D discrete time signal	6
1.2	2-D Kronecker Signal	7
1.3	2-D Unit step	8
1.4	2-D shift invariance example	9
1.5	N-D discrete time system	10
1.6	Direct form I.	21
1.7	Block diagram representation of the cascade form.	21
1.8	Lattice N-order realization.	23
2.1	Block diagram of a 2-D transfer function with factorable numerator.	35
3.1	The proposed lattice- ladder 2-D digital filter with two basic lattice sections.	41
3.2	The proposed lattice- ladder 2-D digital filter with NxM basic lattice sections.	42
3.3	Lattice- ladder 2-D digital filter with N=2 and M=1.	46
3.4	3-D first order FIR lattice structure.	47
3.5	The proposed 3-D recursive lattice structure.	49
3.6	The proposed generalized 3-D recursive digital all-pass filter with order $N \times N \times N$	50
4.1	The magnitude response of 1D notch filter $\ H(e^{j\omega})\ $	55
4.2	Lattice second-order all-pass filter.	57
4.3	The magnitude response of notch filter ($\ H_n(e^{j\omega})\ $) and perfect resonant filter ($\ H_r(e^{j\omega})\ $).	58
4.4	The proposed Lattice-ladder 2-D digital filter.	59
4.5	The proposed 2-D IIR Notch Filter structure.	61
4.6	The parallel 2-D IIR Notch Filter structure.	63

4.7	The magnitude response of 2D notch filter $\ H_{n1}(e^{j\omega_1}, e^{j\omega_2})\ $. . .	64
4.8	The magnitude response of 2D notch filter $\ H_N(e^{j\omega_1}, e^{j\omega_2})\ $. . .	65
4.9	(a) The magnitude response of 2-D notch filter $\ H_N(e^{j\omega_1}, e^{j\omega_2})\ $, (b) The loss $(1 - \ H_N(e^{j\omega_1}, e^{j\omega_2})\)$ of the designed notch filter ,with $(\omega_{1N}, \omega_{2N}) = (-0.5\pi, 0.5\pi)$	66
4.10	Example of single sinusoidal interference removal. (a) Original image (b) Corrupted image (c) Image with interference DFT magnitude (d) Image restored by using 2-D IIR notch filter $\ H_N(e^{j\omega_1}, e^{j\omega_2})\ $	67
4.11	Proposed 3-D recursive digital all-pass filter with order $1 \times 1 \times 1$.	69
4.12	Implementation of $H_p(z_1, z_2, z_3)$	70
4.13	The rejection bandwidth can be adjusted by varying the coeffi- cient k_2	70
4.14	First order 3-D inductance resistance system.	71
4.15	The 3-D IIR notch filter design.	72
4.16	Three-dimensional magnitude response with the notch fre- quency is $(-0.6\pi, 0.5\pi, -0.4\pi)$. (a) $\omega_3 = -0.8\pi$. (b) $\omega_3 = -0.6\pi$. (c) $\omega_3 = -0.4\pi$. (d) $\omega_3 = -0.2\pi$	74

Introduction

The linear time invariant LTI systems form a very simple class of systems that can be analyzed rather easily and for which many analytic and numerical results are available, and have been used to solve many problems that appear in practice in a very satisfactory way. The fact that most physical systems have real inputs and by the fact that some concepts have a more natural physical interpretation for discrete-time systems than for continuous-time systems. Furthermore, most of the techniques for discrete-time systems with real-valued inputs and outputs are also valid for systems with complex inputs and outputs and for continuous-time systems. The minimal state-space realization problem starting from impulse responses (or more general: sequences of Markov parameters) has been studied since the early 1960s and many algorithms have been developed to solve the problem of linear system. The aim of the minimal state space realization problem is to find a state space model of minimal size of the given system. Moreover, minimal realization techniques can also be used to reduce the order of existing state space models. In general the minimal state-space realization problem for LTI systems can be formulated as follows: Given some data about an LTI system, find a state-space description of minimal size that explains the given data. The data are typically the impulse response of the system, the step response, input output measurements, frequency response data, or more general frequency measurements, It can encode to multi-dimensional systems. In this thesis we will give definitions of the basic minimal state-space realization methods, and focus on the minimal state-space realization in multidimensional systems [19, 22, 33]. The main subject of this thesis is in the crucial problem of constructing state-space realizations of 2-D/3-D linear systems from proposed structures in lattice and ladder-lattice form. We use this proposed structures on lattice and ladder-lattice to design 2-D/3-D digital notch filters.

In this thesis, chapter 1 includes basic definitions, facts and examples of multidimensional signals and systems, chapter 2 describe some methods of the minimal realization and an example in the literature of the multidimensional minimal state space realization, chapter 3 discusses the minimal realization in multidimensional systems of proposed structures in lattice and lattice-ladder form, chapter 4 explain the design of notch filters in 2-D and 3-D system based on the proposed lattice and lattice-ladder structures. In chapter 5 ,conclusion. In order to limit the already large number of refer-

ences in the bibliography of this these we have selected a small subset of possible references.

Chapter 1

Multi-dimensional signals and systems

1.1 Introduction

In signal processing (M-D) multidimensional signal processing covers all signal processing done using M-D signals and systems. While multidimensional signal processing is a subset of signal processing, it is unique in the sense that it deals specifically with data that can only be adequately detailed using more than one dimension. In M-D digital signal processing, useful data is sampled in more than one dimension. Variety of examples ranging from image processing and multi-sensor radar detection. These examples use multiple sensors to sample signals and form images based on the manipulation of these multiple signals. The design and implementation in (M-D) requires more complex algorithms, compared to the 1-D case [19]. A multidimensional signal is similar to a single dimensional signal as far as manipulations that can be performed, such as sampling, Fourier analysis, and filtering. The actual computations of these manipulations grow with the number of dimensions [71].

1.2 Multi-dimensional signals

Signals arise in almost every areas of science and engineering such as radar, sonar, communication, medical signal processing, astronomy, acoustics, biology, seismology, telemetry, and economics to name just a few. We are

very interested in natural and man-made signals, the latter make it possible for us to talk to one another over vast distances, enable the diffusion of huge amounts of information over the Internet, instruct robots how to perform very intricate tasks rapidly [19].

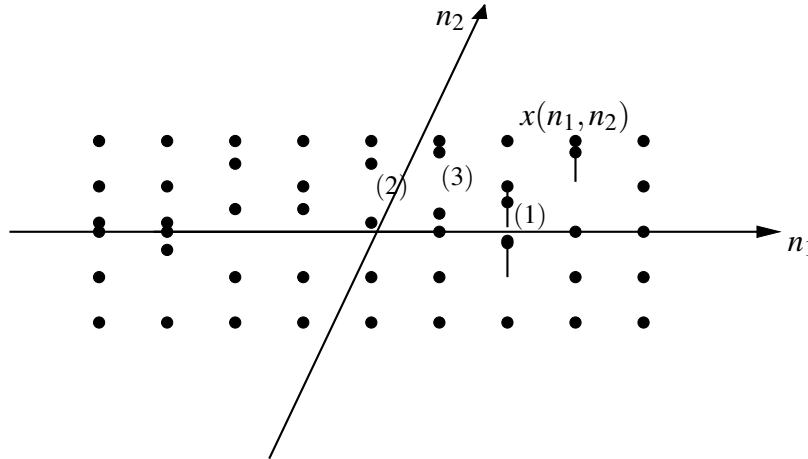


Fig. 1.1 2-D discrete time signal

Also, the market indices can help us determine whether it is the right time to invest and, if so, what type of investment should we go for.

A N-D signal, is a physical or contrived quantity that depends on N real independent integer variables (n_1, n_2, \dots, n_N) . It can be represented by a function $x(n_1, n_2, \dots, n_N)$, where (n_1, n_2, \dots, n_N) , may represent time, distance, ..etc. A scalar N-D signal $x(\vec{n})$ where $(\vec{n}) = (n_1, n_2, \dots, n_N)$, $x(\vec{n})$ is mathematically a complex N-sequence, or a mapping of the N-D integers into the complex plane. Our convention is that the signal s is defined for all finite values of its integer arguments (\vec{n}) using zero padding as necessary. Occasionally we will deal with finite-extent signals, but will clearly say so. We will adopt the simplified term sequence over the more correct N-sequence [19, 71]. An example of 2-D signal is shown in figure 1.1.

1.2.1 Kronecker delta function

A simple example of a N-D signal is the impulse $\delta(\vec{n})$, it is zero everywhere except (\vec{n}) equals zero [71]

$$\delta(\vec{n}) = \begin{cases} 1 & (\vec{n}) = (\vec{0}), \\ 0 & \text{otherwise.} \end{cases}$$

a portion of 2-D impulse signal is plotted in figure 1.2.

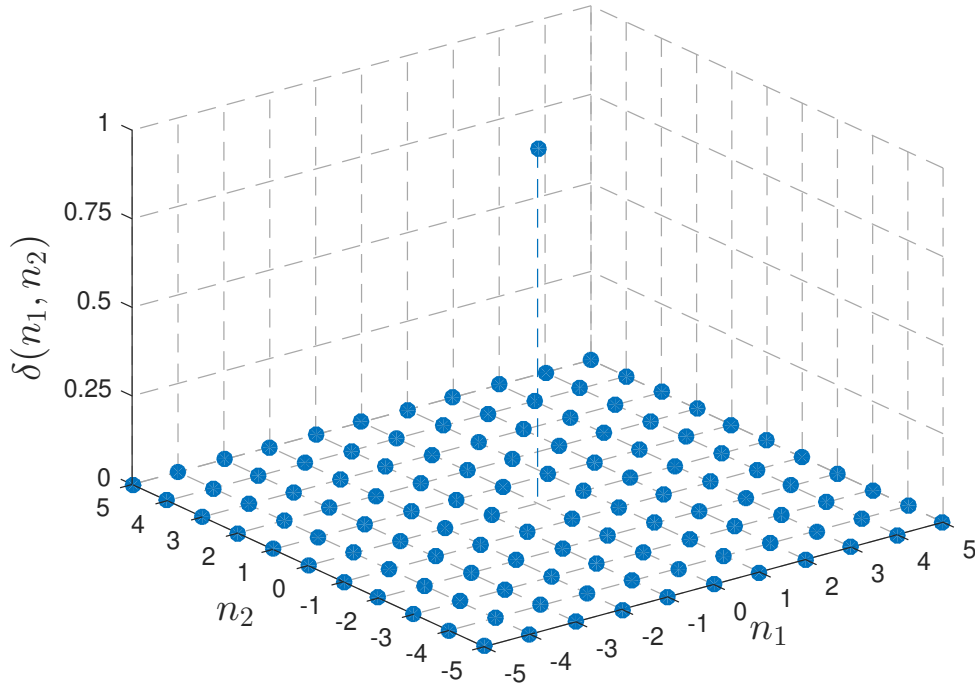


Fig. 1.2 2-D Kronecker delta function

1.2.2 The Heaviside step function

The unit step function, usually denoted by H or u , **1** a discontinuous function, named after Oliver Heaviside, whose value is zero for negative arguments and one for positive arguments. $u(\vec{n})$ is also an important signal which is presented by [71]:

$$u(\vec{n}) = \begin{cases} 1 & (n_1 \geq 0, n_2 \geq 0, \dots, n_N \geq 0) \\ 0 & \text{otherwise.} \end{cases}$$

Figure 1.3, show a 3-D unit step function and can presented by

$$u(n_1, n_2, n_3) = \begin{cases} 1 & (n_1 \geq 0, n_2 \geq 0, n_3 \geq 0) \\ 0 & \text{otherwise.} \end{cases}$$

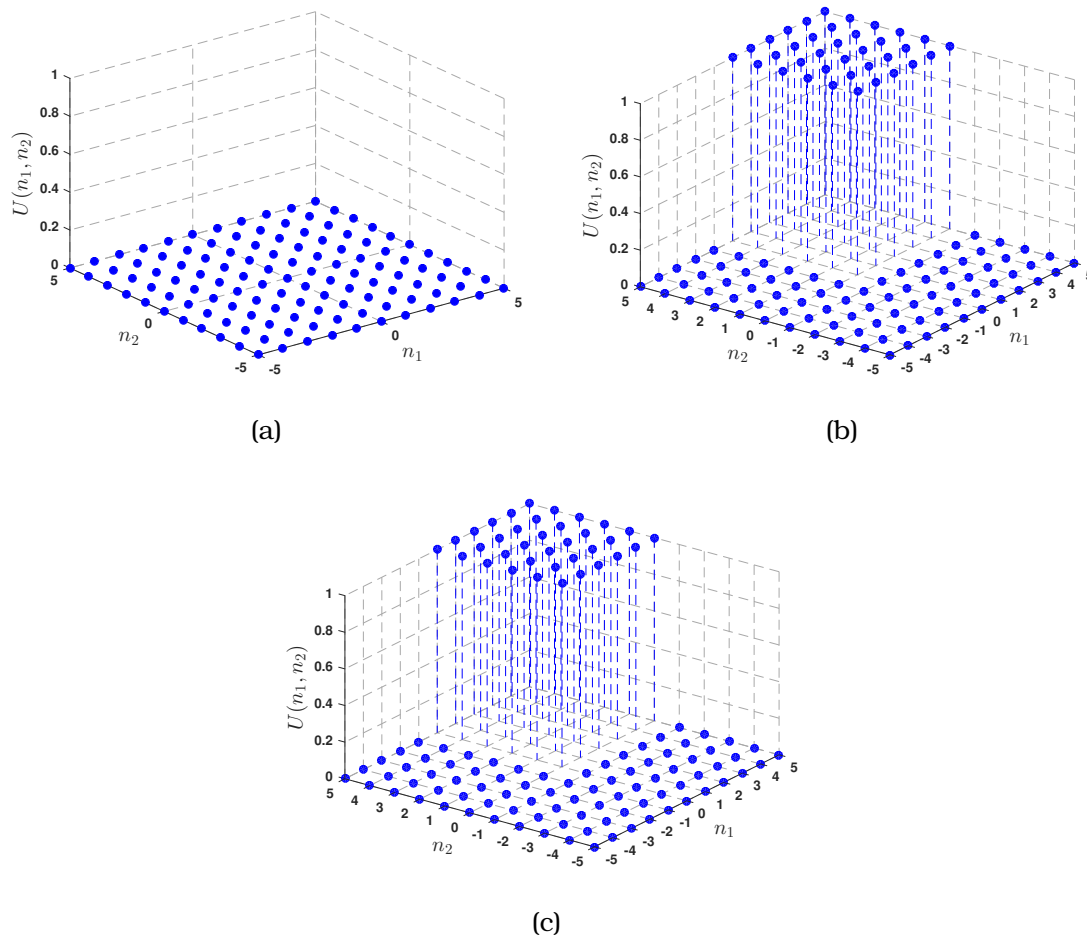


Fig. 1.3 3-D Heaviside step function (a) $n_3 < 0$, (b) $n_3 = 0$, (c) $n_3 > 0$

1.2.3 Separable sequence

$x(\vec{n})$ is a separable sequence if it can be written as

$$x(\vec{n}) = \prod_{i=1}^N x_i(n_i),$$

where $x_i(n_i)$ are N -sequences of one variable n_i respectively. Any sequence that can be expressed as the product of 1-D sequences in this form is to be said separable. Separable sequences can be quite valuable when used as test inputs for evaluating and debugging experimental systems. Signals may be combined by a variety of operations which will serve as building blocks for the development of more complicated systems [41].

1.2.4 Linearity

Let $x_1(n_1, n_2, \dots, n_N)$ and $x_2(n_1, n_2, \dots, n_N)$ represent N-D discrete signals, these signals can be added to yield a new signal, the addition is performed sample by sample.

$$y(n_1, n_2, \dots, n_N) = x_1(n_1, n_2, \dots, n_N) + x_2(n_1, n_2, \dots, n_N)$$

N-D sequences may be multiplied by a constant to form a new sequence. If we let c_1 represent a constant, we can form the N-D sequence $y(n_1, n_2, \dots, n_N)$ from the scalar c_1 and the sequence $x(n_1, n_2, \dots, n_N)$ by multiplying each sample value of x by c_1

$$y(n_1, n_2, \dots, n_N) = c_1 x(n_1, n_2, \dots, n_N)$$

1.2.5 Shift invariance

[19, 71, 14] A N-D sequence $x(\vec{n})$ where $(\vec{n}) = (n_1, n_2, \dots, n_N)$ may also be linearly shifted to form a new sequence $y(\vec{n})$. The operation of shifting simply slides the entire sequence $x(\vec{n})$ to a new position in the (\vec{n}) plane. The sample values of $y(\vec{n})$ are related to the sample values of $x(\vec{n})$ by [41]:

$$y(\vec{n}) = x(\vec{n} - \vec{m}),$$

where (\vec{m}) is the amount of the shift, and $(\vec{n} - \vec{m}) = (n_1 - m_1, n_2 - m_2, \dots, n_N - m_N)$. An example of sequence shifting 2-D appears in figure 1.4

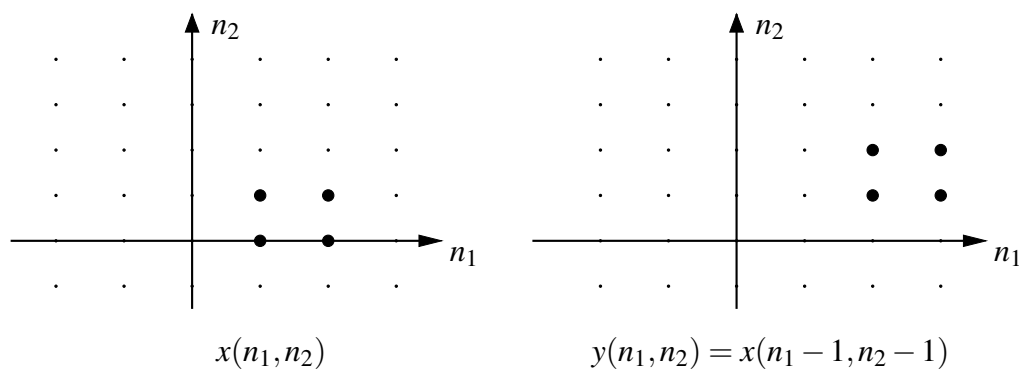


Fig. 1.4 2-D shift invariance example

Using the fundamental operations of addition, scalar multiplication, and shifting, it is possible to decompose any N-D sequence into a sum of weighted and shifted N-D unit impulses.

1.3 Multidimensional systems

Multidimensional systems are the necessary mathematical background for modern digital image processing with many applications in biomedicine, X-ray technology and satellite communications [19]. Although digital filtering in several dimensions is gaining importance in medicine, heart volume measurements, in fire control problems, and to analyze complex electronic circuitry, there exists no general theory concerning structures, analysis and design. In mathematical systems theory, a m-D system is an operator transforming an input into an output in which not only one independent variable exists, but there are several independent variables. The operator embodied in this system is described by $T[\cdot]$, as illustrated in figure 1.5, so we can write [41]

$$y(n_1, n_2, \dots, n_N) = T[u(n_1, n_2, \dots, n_N)]$$

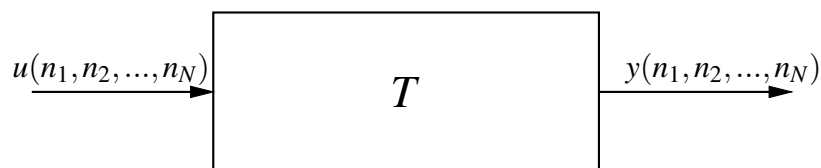


Fig. 1.5 N-D discrete time system

The operator $T[\cdot]$ can represent a rule or a set of rules for mapping an input signal into an output signal, or even a list of output signals that correspond to various input signals. In this these we focus our attention on linear shift-invariant systems and theirs characterizations. Before we get that far, however, we shall discuss some simple operations that can be performed on multidimensional discrete signals.

1.4 Fundamental operations on Multidimensional system

1.4.1 Linear system

A system is said to be linear if and only if it satisfies two conditions: if the input signal is the sum of the two sequences, the output signal is the sum

of the output corresponding output sequences, and scaling the input signal produces a scales output signal. Therefore, if $L[.]$ denoted the linear operator system and $(\bar{n}) = (n_1, n_2, \dots, n_N)$ [41]

$$y_1(\bar{n}) = L[x_1(\bar{n})], y_2(\bar{n}) = L[x_2(\bar{n})]$$

then

$$L[\alpha x_1(\bar{n}) + \beta x_2(\bar{n})] = \alpha y_1(\bar{n}) + \beta y_2(\bar{n})$$

for all input signals and all complex constants α and β , linear systems obey the principale of superposition. The response of linear system to a weighted sum of input signals is equal to the weighted sum of the responses to the individual input signals.

1.4.2 Shift invariant systems

A system $T[.]$ is shift-invariant if any shift of an arbitrary input $x(\bar{n})$ produces the identical shift in the corresponding output $y(\bar{n})$. If $T[x(\bar{n})] = y(\bar{n})$, then for all (integer) shifts (\bar{m}) we have $T[x(\bar{n} - \bar{m})] = y(\bar{n} - \bar{m})$ for all sequences $x(\bar{n})$

1.4.3 Convolution

A linear shift-invariant system is completely characterized by its unit sample response $h(\bar{n})$, the response to the input $x(\bar{m})$ is [41]

$$y(\bar{n}) = \sum_{\substack{\bar{m} \\ (-\infty \leq m_i \leq \infty)}} \sum \dots \sum x(\bar{m}) h(\bar{n} - \bar{m}) = \sum_{\substack{\bar{m} \\ (-\infty \leq m_i \leq \infty)}} \sum \dots \sum h(\bar{m}) x(\bar{n} - \bar{m}). \quad (1.1)$$

where

$$\sum_{\substack{\bar{m} \\ (-\infty \leq m_i \leq \infty)}} \sum \dots \sum = \sum_{m_1=-\infty}^{\infty} \sum_{m_2=-\infty}^{\infty} \dots \sum_{m_N=-\infty}^{\infty}$$

Equation (1.1) defines N-Dimensional convolution and will also be represented by

$$y(n) = x(\bar{n}) * h(\bar{n})$$

1.4.4 Properties of N-D convolution

- Commutativity $x * y = y * x$.
- Associativity $(x * y) * z = x * (y * z)$.
- Identity element $\delta(\vec{n})$ with property $\delta(\vec{n}) * x = x$.
- Zero element: $0(\vec{n}) = 0$ with property $0 * x = 0$.

All of these properties of convolution hold for any N-D signals x , y , and z , for which convolution is defined (i.e., for which the infinite sums exist).

1.5 N-D z-transform

Z-transform maps a function of discrete time \vec{n} to a function of \vec{z} . Although motivated by system functions, we can define a Z-transform form for any N-dimensional input sequence $x(\vec{n})$ by

$$X(\vec{z}) = Z(x(\vec{n})) = \sum_{(-\infty \leq n_i \leq \infty)}^{\vec{n}} \dots \sum x(\vec{n}) z^{-\vec{n}}. \quad (1.2)$$

where $\vec{z} = (z_1, z_2, \dots, z_N)$, $(z^{-\vec{n}} = z_1^{-n_1} z_2^{-n_2} \dots z_N^{-n_N})$, and the z_i are complex variables, which, expressed in polar form

$$z_i = r_i e^{j\omega_i}$$

where ω_i is the i^{th} spatial frequency variable and can be used to rewrite (1.2) as

$$X(\vec{z}) = Z(x(\vec{n})) = \sum_{(-\infty \leq n_i \leq \infty)}^{\vec{n}} \dots \sum x(\vec{n}) (r_1^{-n_1} e^{-jn_1\omega_1}) (r_2^{-n_2} e^{-jn_2\omega_2}) \dots (r_N^{-n_N} e^{-jn_N\omega_N}). \quad (1.3)$$

Similarly to the one-dimensional case, the N-Dimensional Z-transform can be interpreted as the N-Dimensional Fourier transform of $x(\vec{n})$, whenever

$$r_i = |z_i| = 1$$

For convergence of the N-Dimensional Z-transform, the sequence $x(\vec{n})z^{-\vec{n}}$ must be absolutely summable. This is equivalent to

$$\sum_{\substack{\vec{m} \\ (-\infty \leq m_i \leq \infty)}} \sum \dots \sum |x(\vec{n})r^{-\vec{n}}| < \infty. \quad (1.4)$$

The set of z_i , for which (1.4) holds, defines the region of convergence. Notice that because of the multiplication of the sequence $x(\vec{n})$ by $r^{-\vec{n}}$, it is possible for the Z-transform to converge, even if the Fourier transform does not.

1.5.1 Properties of N-D z-transform

The Z-transform operation has a number of properties that can be useful in performing calculation, solving problems, and proving theorems. Below we state several of these properties

Linearity

$$Z(\alpha x(\vec{m}) + \beta y(\vec{m})) \longleftrightarrow \alpha Z(x(\vec{m})) + \beta Z(y(\vec{m})) \quad \text{where } \alpha \text{ and } \beta \text{ are constants.}$$

Delay property

$$\text{If } x(\vec{n}) \longleftrightarrow X(\vec{z}) \text{ for } z \text{ in ROC}$$

$$\text{then } x(\vec{n} - 1) \longleftrightarrow \vec{z}^{-1}X(\vec{z})$$

We have an example of this property

$$\delta(\vec{n}) \longleftrightarrow 1$$

$$\delta(\vec{n} - 1) \longleftrightarrow \vec{z}^{-1} = z_1^{-1} \cdot z_2^{-1} \dots z_N^{-1}$$

Convolution

Convolution is an important computational and conceptual tool: it provides an important new way to think about the behaviors of system. If $y(\vec{n})$ is equal to the convolution of two N-dimensional sequences $x(\vec{n})$ and $h(\vec{n})$, then the Z-transform of $y(\vec{n})$ is equal to the product of the Z-transforms of $x(\vec{n})$ and $h(\vec{n})$,

$$y(\vec{n}) = \sum_{\substack{\vec{m} \\ (-\infty \leq m_i \leq \infty)}} \sum \dots \sum x(\vec{n})h(\vec{m} - \vec{n}). \quad (1.5)$$

then

$$Y(\bar{z}) = X(\bar{z})H(\bar{z}). \quad (1.6)$$

This can easily be seen by writing

$$Y(\bar{z}) = \sum_{(-\infty \leq \bar{n}_i \leq \infty)} \sum \dots \sum \left\{ \sum_{(-\infty \leq \bar{m}_i \leq \infty)} \sum \dots \sum x(\bar{m})h(\bar{n} - \bar{m}) \right\} z^{-\bar{n}}. \quad (1.7)$$

and after interchanging the order of summation ,and changing the indice of summation this becomes

$$Y(\bar{z}) = \sum_{(-\infty \leq \bar{m}_i \leq \infty)} \sum \dots \sum x(\bar{n}) \left\{ \sum_{(-\infty \leq \bar{k}_i \leq \infty)} \sum \dots \sum h(\bar{k}) . z^{-\bar{k}} \right\} z^{-\bar{m}}. \quad (1.8)$$

which is equal to

$$Y(\bar{z}) = X(\bar{z})H(\bar{z}). \quad (1.9)$$

1.5.2 Inverse Z-Transform

The inversion formula for the above transform is given by

$$x(\bar{m}) = \frac{1}{(2\pi j)^N} \oint_{\bar{C}_N} \dots \oint X(\bar{z}) z^{(\bar{m}-\bar{l})} d\bar{z} \quad (1.10)$$

where, N paths and \bar{C}_N are within the regions of convergence of (1.10) and $d\bar{z} = dz_1 . dz_2 \dots dz_N$. This formula follows by substituting $x(\bar{z})$ in (1.8) , which becomes [42].

$$x(\bar{m}) = \frac{1}{(2\pi j)^N} \oint_{\bar{C}_N} \dots \oint \sum_{(-\infty \leq \bar{n}_i \leq \infty)} \sum \dots \sum x(\bar{n}) z^{-\bar{n}} z^{(\bar{m}-\bar{l})} d\bar{z} \quad (1.11)$$

The interchange of summations and integrations, which is justified by the absolute convergence of the series for $X(z)$, yields

$$x(\bar{m}) = \frac{1}{(2\pi j)^N} \sum_{(-\infty \leq \bar{n}_i \leq \infty)} \sum \dots \sum x(\bar{n}) \oint_{\bar{C}_N} \dots \oint z^{(-\bar{n}+\bar{m}-\bar{l})} d\bar{z} \quad (1.12)$$

By the Cauchy Integral Theorem of N-variables and since the paths of integration \bar{C}_N are chosen within the region of convergence, it follows that

$$\oint_{\bar{C}_N} \dots \oint z^{(-\bar{n}+\bar{m}-\bar{l})} d\bar{z} = \begin{cases} (2\pi j)^N, & \text{if } (\bar{m} + \bar{n}) = (\bar{0}) \\ 0, & \text{otherwise} \end{cases} \quad (1.13)$$

1.6 N-D Fourier transform

The Fourier Transform is a mathematical technique that transforms a function of time, to a function of frequency [42]

$$X(\bar{\omega}) = \sum_{\substack{\bar{n} \\ (-\infty \leq n_i \leq \infty)}} \dots \sum x(\bar{n}) e^{-j\bar{n}\bar{\omega}}. \quad (1.14)$$

$$x(\bar{n}) = \int_{\omega_1=-\pi}^{\pi} \dots \int_{\omega_N=-\pi}^{\pi} X(\bar{\omega}) e^{j\bar{\omega}\bar{n}} d\bar{\omega} \quad (1.15)$$

where, $(e^{\bar{n}\bar{\omega}} = e^{n_1\omega_1} \dots e^{n_N\omega_N})$, $d\bar{\omega} = d\omega_1 \dots d\omega_N$

1.7 Stability

1.7.1 BIBO stability

Stable systems are those for which a small change in the input gives a small change in the output [19, 71, 14]. As such, they are very useful in applications. We can mathematically define bounded-input bounded-output (BIBO) stability for N-D systems analogously to that in 1-D system theory. A spatial or N-D system will be stable if every bounded (finite) input produces a bounded (i.e., finite) output. For linear time-invariant digital filters, a necessary and sufficient condition for stability is

$$S = \sum_{\substack{\bar{n} \\ (-\infty \leq n_i \leq \infty)}} \dots \sum |h(\bar{n})| < \infty. \quad (1.16)$$

Theorem 1-1 A N-D LSI system is BIBO stable if and only if its impulse response $h(\bar{n})$ is absolutely summable

Proof: See Appendix A.

1.7.2 Necessary and sufficient conditions stability in N-Dimensions

A stability region is said to be convex if the loci of all points connecting two stable points lies inside the stable region. It is well known that the stability area for a second order one-dimensional transfer function satisfies convexity, but it can be shown that the stability region of the third order one-dimensional transfer function is not convex. It is, therefore, conjectured that the bounding surfaces of a multi-dimensional higher order filter stability region cannot be described in terms of plane surfaces which explains why the following method to derive necessary and sufficient stability conditions is rather complicated to apply. The advantage of this approach lies in the fact that the method must be applied only once for a particular type of transfer function, which results in a set of stability conditions. These conditions can be easily applied by the design engineer [41].

1.7.3 Method to derive necessary and sufficient stability conditions

The method to derive necessary and sufficient stability conditions consists of two steps:

- Derive necessary and sufficient conditions for one variable polynomial with complex coefficients using Rouché's theorem.
- Apply the following theorem and corollary to state necessary and sufficient conditions for N-Dimensions

Theorem 1-2: [44] Let $(\delta_1, \delta_2, \dots, \delta_N)$ be any N-tuple of complex numbers such that $r = \max|\delta_i| \leq 1$. Then $Q(z_1, \dots, z_N)$ is stable if and only if for all $\bar{\delta}$ the polynomial

$$q_{\bar{\delta}}(z) = Q\left(z\frac{\delta_1}{r}, \dots, z\frac{\delta_N}{r}\right)$$

is stable.

Proof: See Appendix B.

Corollary 1 :The polynomial $Q(\bar{z})$ corresponds to a stable transfer function if and only if for all complex numbers $\bar{\delta}$ such that $\max|\delta_i| = 1, q_{\bar{\delta}}(z) = Q(z\delta_1, \dots, z\delta_N)$ is stable.

Proof: See Appendix B.

1.8 State-space models and transfer function

As in the 1-D case, state space models are a very important class of internal representations. In this context, the concept of the state of a system can be defined as the memory of the system, i.e. the past and future evolutions are independent given the current state. Furthermore, a state space is a mathematical model of a physical system as a set of input, output and state variables. Commonly used models for systems recursive are the Roesser model (Roesser (1975)) and the Fornasini-Marchesini models. There are several N-D state-space models such as Fornasini- Marchesini, Attasi and Roesser, but in this work we focus on the Rosser's model [22].

1.8.1 Givone-Roesse's model

The intrinsic feature of the Givone-Roesse model is that the partial state vector is partitioned into n sub-vectors for n -D systems. For 2-D systems these fractions are called the vertical and the horizontal state sub-vectors. A Roesser state-space model of N-D digital filter can be represented as [22, 56]

$$x(\bar{n}) = [x_1(\bar{n})^T, x_2(\bar{n})^T, \dots, x_N(\bar{n})^T]^T$$

$$\begin{bmatrix} x(n_1 + 1, n_2, \dots, n_N) \\ x(n_1, n_2 + 1, \dots, n_N) \\ \dots \\ x(n_1, n_2, \dots, n_N + 1) \end{bmatrix} = Ax(\bar{n}) + Bu(\bar{n}), \quad (1.17)$$

$$y(\bar{n}) = Cx(\bar{n}) + Du(\bar{n}), \quad (1.18)$$

$x(\bar{n}) \in \mathbb{R}^n$, where, $(\bar{n}) = (n_1, n_2, \dots, n_N)$, $u(\bar{n})$ and $y(\bar{n})$ are the scalar input and output of the filter respectively (A, B, C, D) are real coefficient matrices with suitable size. In particular, $A \in \mathbb{R}^{n \times n}$. The state-space (1.17, 1.18) is also conventionally denoted by (A, B, C, D) . The transfer function of (1.17, 1.18) is [21]

$$H(z_1, z_2) = CZ(I_n - AZ)^{-1}B + D, \quad (1.19)$$

where $Z = \text{diag}\{z_1 I_n, z_2 I_n, \dots, z_n I_n\}$ and I_n the $n \times n$ identity matrix.

1.8.2 Recursive equation

An important subclass of linear, shift-invariant N-Dimensional filters is constituted of those systems for which the input and output satisfy a linear, constant coefficient difference equation of the form [41]:

$$y(\vec{n}) = \sum_{\substack{\vec{m} \\ (-\infty \leq m_i \leq \infty)}} \sum \dots \sum a_{(\vec{m})} y(\vec{n} - \vec{m}) + \sum_{\substack{\vec{l} \\ (-\infty \leq l_i \leq \infty)}} \sum \dots \sum b_{(\vec{l})} x(\vec{n} - \vec{l}). \quad (1.20)$$

where

$$\sum_{i=1}^N m_i \neq 0 \quad (1.21)$$

with $a_{(\vec{m})} = a_{(m_1, \dots, m_N)}$ and $b_{(\vec{l})} = b_{(l_1, \dots, l_N)}$ are the sets of constant coefficients which characterize a particular filter. Equation (1.20) does not uniquely specify the input-output relationship of a system. This is a consequence of the fact that as with differential equations, a family of solutions may exist. Therefore, a set of initial conditions must also be specified. It is assumed that if a system satisfies a linear constant coefficient N-Dimensional difference equation, it will also be shift-invariant. If the set of all $a_{(\vec{m})}$ is non-empty for all m_i such that

$$\sum_{i=1}^N m_i \neq 0,$$

then (1.20) characterizes a recursive system algorithm and may be used as a computational realization of the system, either by programming a general purpose digital computer or by implementation using special purpose hardware.

1.8.3 Transfer function

Taking the Z-transform of the N-Dimensional linear difference equation, (1.20), leads to

$$Y(\vec{z}) = H(\vec{z}) X(\vec{z}). \quad (1.22)$$

where

$$H(\vec{z}) = \frac{\sum_{\substack{\vec{l} \\ (-\infty \leq l_i \leq \infty)}} \sum \dots \sum b_{(\vec{l})} z^{-\vec{l}}}{1 - \sum_{\substack{\vec{m} \\ (-\infty \leq m_i \leq \infty)}} \sum \dots \sum x(\vec{n}) a_{(\vec{m})} z^{-\vec{m}}}. \quad (1.23)$$

$$\sum_{i=1}^N m_i \neq 0,$$

Note

$$\sum_{i=1}^N m_i = 0 \quad \text{implies} \quad m_1 = 0, \dots, m_N = 0$$

The order of $H(\bar{z})$ is defined as the sum of all M_i

1.8.4 Differences between transfer functions and state-space models

The authors in [60, 11] cite the important differences between the transfer function and the state-space representation. The transfer function of an LTI system is the relationship between input and output of the system.

- The transfer function formulation does not reveal the behavior inside the system, such as unobservable unstable modes. Therefore, the transfer function matrix cannot always be used to study the stability properties of an LTI system. This problem of hidden pole-zero cancellation was not really understood prior to the work of [24, 34], who proved that the input/output description reveals only the controllable and observable part of a dynamical system [19].
- In practice the state-space formulation is very important for numerical computations and controller design, the state-space formulation stays the most elegant way of dealing with generalizations.
- The state-space formulation can easily be extended to the time-varying case. The extension of the transfer function to the time-varying case has not been very successful.

1.9 N-Dimensional digital filter

A digital filter is defined to be an algorithm by which a digital signal or equivalently a sequence of numbers acting as input, is transformed into a second sequence of numbers or output digital signal, where, the term 'digital' implies that both time (the independent variable) and amplitude are quantized [19]. In many applications, continuous signals are encountered that are functions of (\bar{n}) independent variables, say (n_1, n_2, \dots, n_N) . N-Dimensional signals of this type can be represented by functions of the form $x(\bar{n})$. Each of

variables can represent an arbitrary physical quantity such as time, length, velocity, acceleration, and temperature. The well-known methods of the synthesis of N-Dimensional filters are considered in a number of literature [18, 19, 1] and monographs. The simplest considered method is one of a cascading of (\bar{n}) one-dimensional filters, for which the pass band region of synthesized filter is an N-Dimensional parallelepiped with scaled cut-off frequencies. The great possibilities present the synthesis method based on using the reactance function with subsequent bilinear transformation of variables. The method leads to the synthesis of N-Dimensional filters with scaled cut-off frequencies and regulated convexity of the pass band region.

1.10 Realization of digital filters

Once we have obtained the transfer function of an FIR or IIR filter that approximates the desired specifications in the frequency domain or the time domain. A given transfer function can be realized by several structures or what we will call (circuits), and they are all equivalent in the sense that they realize the same transfer function under the assumption that the coefficients of the transfer function have infinite precision. But in reality, the algorithms for implementing the transfer function in hardware depend on the filter structure chosen to realize the transfer function. We consider different structures for realization of a digital filter

1.10.1 Direct form I

For convenience in showing the realization, the order of the numerator and denominator are set to be the same. Direct form 1 uses separate delays for both the numerator polynomial and the denominator polynomial. In certain cases, e.g., floating-point additions, the results may depend on the exact ordering in which the additions are performed, and shown in figure.1.6

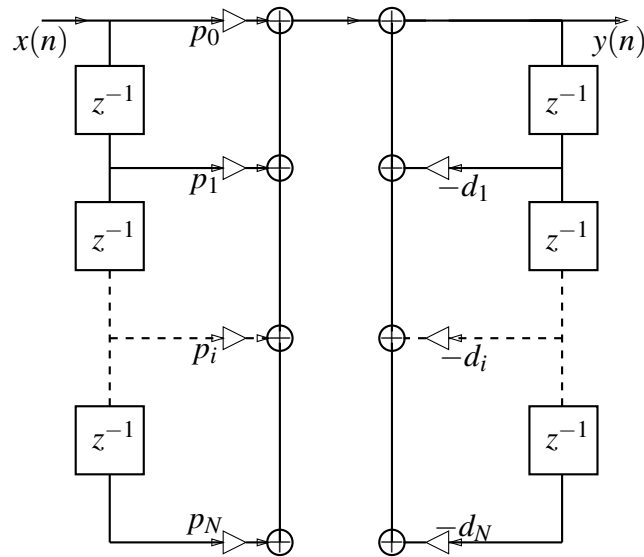


Fig. 1.6 Direct form I.

1.10.2 Direct form II

Direct form 2 has been called the canonic form because it has the minimum number of multiplier, adder, and delay elements, but since other configurations also have this property. Direct form 2 uses the same delays for both the numerator polynomial and the denominator polynomial.

1.10.3 Cascade Realization

The cascade implementation of a filter is obtained by expressing the filter transfer function $H(z)$ in a factorized form, which is shown in figure.1.7, where

$$H(z) = \prod_{i=1}^k H_i(z),$$

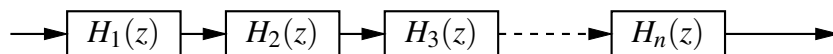


Fig. 1.7 Block diagram representation of the cascade form.

1.10.4 Parallel Realization

To produce Parallel form of the IIR filter structure, the numerator and denominator of the factorized system will be split into summation form such as

$$H(z) = \sum_{i=1}^k H_i(z)$$

And we can use the partial fraction method, in a parallel form as parallel sum of a number of second order and first order terms.

1.10.5 Lattice and ladder realisation

Lattice filters are used extensively in digital speech processing and in the implementation of adaptive filters. Lattice filter structures can be used to implement FIR and IIR filters. Lattice coefficients can be derived from the coefficients of the transfer functions with some algebra with a method called lattice realization method of Gray and Markel [28]. This is based on the configuration depicted in figure 1.8. A typical application of lattice filters is in linear prediction for speech processing. They can be used to model the vocal tract with an all-pole structure. A lattice filter is the most efficient structure for generating at the same time the forward and backward prediction errors. The networks represented by the blocks in figure 1.8 can assume a number of distinct forms. The structure have several desirable features as follows

- The synthesis procedure is very efficient. Only on the order of M^2 operations are necessary for the synthesis. No polynomial root solvers or explicit simultaneous equation solvers are necessary.
- A built-in stability test exists within the synthesis process. If any k -parameter magnitude exceeds or equals unity, the filter is unstable. Otherwise, it is stable.

• All stable recursive filters can be transformed into the forms presented. Also, the lattice structure is modular: increasing the order of the filter requires adding only one extra module, leaving all other modules the same. In lattice filter implementations of fixed-point IIR filters, stability and frequency responses are less sensitive to round-off errors of the coefficients compared to classic implementations. This means that coefficients of lattice filters require fewer bits than the coefficients of IIR filters implemented with direct forms.

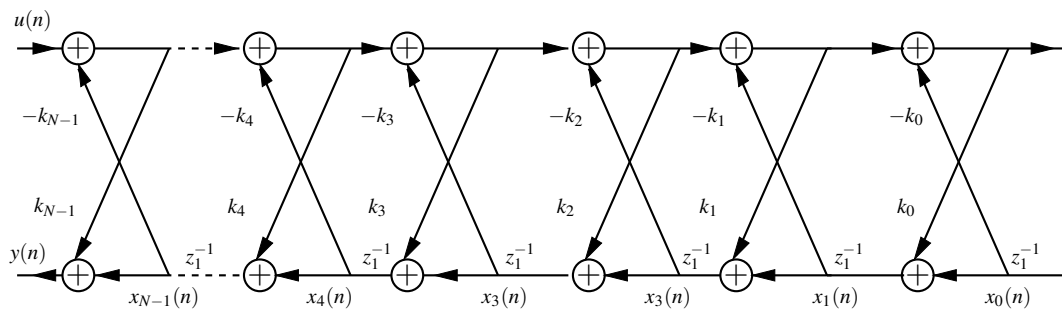


Fig. 1.8 Lattice N-order realization.

1.11 Conclusion

In this chapter definitions, the properties of N-D z-transform, stability, state-space, transfer function of multidimensional systems was presented. The realization of digital filters direct form, cascade and parallel realization are defined. The lattice and ladder lattice form which combines features will be used to develop compact realization of 2-D and 3-D notch filters. Also, this chapter includes facts and examples of multidimensional signals and systems.

Chapter 2

Minimal state-space realization in linear systems

2.1 Introduction

Linear systems have been under study for a long time, and from several different points of vision, in physics, mathematics, engineering and many other areas. But the subject is such a fundamental, and deep one that there is no doubt that linear systems will continue to be an object of study for as long as one can divine. However, a particular feature of recent engineering studies focus on the structure of finite dimensional linear systems. While such systems have been extensively studied, especially since 1930s, the frequency domain techniques that were commonly used often did not specifically exploit the underlying finite dimensionality of the systems involved. Moreover, almost all this work was for single-Input, single-output [34] systems and did not seem to extend satisfactory to the multi-input, multi-output systems that become increasingly important in aerospace, process control, and econometric applications in the late 1950s. until 1970s Popov and Rosenbrock [57] have shown that many of the scalar transfer function concepts developed for SISO systems could also be extended to matrix transfer functions for MIMO systems. Now we could say that transfer functions descriptions (which are basically frequency domain methods) and state-space descriptions (which are more oriented towards the time domain) are only two extremes of a whole spectrum of possible descriptions of finite-dimensional LTI systems. We can work exclusively with one description or the other, but we can also easily

translate results from one framework to another, and it really depends on the application we have in mind which method best suits our needs. The purpose of this chapter is to describe some methods for the reduction of nonminimal state-space realizations and for the minimal state-space realization of infinite or finite sequences of Markov parameters of linear time-invariant systems and minimal state-space realization of multidimensional systems.

2.2 The minimal state-space realization problem for LTI systems

The origins of the minimal state-space realization problem lie in the early 1960s. The minimal state-space realization problem for (continuous) LTI systems was first stated by Gilbert [24] and Kalman [34]. Gilbert gave an algorithm for transforming a transfer function into a system of differential equations, this approach of Gilbert was based on partial-fraction expansions. Kalman's algorithm was based on the theory of controllability and observability and reduced a nonminimal state-space realization until it became minimal. Then Kalman and Ho [29, 76] solved the problem starting from the sequence of Markov parameters of the system. All these algorithms assume that the entire sequence of Markov parameters is available. However, many times only a limited number of Markov parameters is available. The corresponding minimal partial state-space realization problem for MIMO systems was first explored by Kalman and Tether [66]. Later, Rissanen [55] gave a recursive solution of the SISO version of this problem (which he claims can easily be extended to the MIMO case). Nevertheless, there are several reasons why the minimal state-space realization problem for LTI systems deserves to be studied:

- This problem is one of the most fundamental problems in system theory and can be considered as a simplified version of problems with noisy data, nonlinear models, etc. that occur frequently in practice. Before we deal with these more complex problems, it is useful to study the simplified version, which might lead to additional insight in the original problems. As such the solution of the minimal state-space realization problem can also be seen as the first step towards problems such as model reduction and identification, which are of important practical interest.

- In order to analyze systems it is advantageous to have a compact description of the system. The aim of the minimal state-space realization problem is to find a state-space model of minimal size of the given system. Moreover, minimal realization techniques can also be used to reduce the order of existing state-space models.
- The minimal realization is both controllable and observable, it is a good basis for designing an observer to estimate the states of the system from measurements of the outputs, and also for subsequently designing a state feedback controller (using e.g. pole placement).
- Furthermore, the minimal state-space realization problem can be solved very elegantly using linear matrix algebra methods, that can be implemented in a numerically stable way.

2.3 Linear time-invariant systems

The evolution of a discrete-time LTI system can be described by a model of the form

$$x(n+1) = Ax(n) + Bu(n), \quad (2.1)$$

$$y(n) = Cx(n) + Du(n), \quad (2.2)$$

with $A \in \mathbb{R}^{n \times n}$, $B \in \mathbb{R}^{n \times m}$, $C \in \mathbb{R}^{l \times n}$ and $D \in \mathbb{R}^{l \times m}$, and where u, y and x are the input, the output and the state respectively. Model (2.1,2.2) are called state-space model. The number of components of the state vector x is called the order of the model. A state-space model will be represented by the 4-tuple (A, B, C, D) of system matrices. The Markov parameters G_k of an LTI system are defined by

$$G_0 = D \quad \text{and} \quad G_k = CA^{k+1}B \quad \text{for} \quad k = 1, 2, \dots \quad (2.3)$$

We say that (A, B, C, D) is a realization of the sequence $\{G_k\}_{k=0}^{\infty}$ if (2.3) holds. The realization is minimal if the model order is minimal. The model order of a minimal realization is called the minimal system order or sometimes also the McMillan degree of the system.

We can cite the minimal state-space realization methods and their related extensions as follows:

2.4 Minimal realization based on reduction of nonminimal realizations

Suppose that we have a (not necessarily minimal) n th-order state-space realization (A, B, C, D) of a given LTI system. Rosenbrock [57] has developed a procedure to transform this realization into a minimal realization. In fact, this algorithm is merely a small modification to the standard algorithm for reducing matrices to echelon form [46].

2.5 Minimal realization of impulse responses

We consider the problem of constructing a minimal realization starting from the impulse response $\{G_k\}_{k=0}^{\infty}$ of the system. Note that we always have $D = G_0$. Therefore, the problem of reconstructing D can be separated from the construction of A, B and C . Many algorithms for minimal state-space realization of impulse responses use the block Hankel matrix [29, 76, 59, 74].

2.6 The minimal partial realization problem

Now we assume that : the transfer function is known exactly, there are an infinite number of Markov parameters available and the underlying system is finite dimensional. So given a finite sequence $\zeta_N = \{G_k\}_{k=0}^N$ we want to find a 4-tuple (A, B, C, D) such that $D = G_0$ and $CA^{k-1}B = G_k$ for $k = 1, 2, \dots, N$. In that case we say that (A, B, C, D) is a partial realization of ζ_N . Note that trivially we have $D = G_0$. The 4-tuple (A, B, C, D) is said to be a minimal partial realization of ζ_N if and only if the size of A is minimal among all other partial realizations of ζ_N [67].

2.7 Minimal realization based on step response data

In many industrial processes we have step response measurements available instead of impulse response data. A straightforward way to do the realization then is to construct impulse response data by differencing or differentiating

the step response data. However, this operation is not attractive since it will introduce an amplification of high-frequency noise in the data. As an alternative approach for discrete-time LTI systems, it is possible to use the step response data directly in a realization method that is a modified version of the Kung method. This modification is due to van Helmont et al. In practice, the measurements that are available will not necessarily be impulse response or step response data, but general input-output data [23].

2.8 Rational approximation

If we apply the z -transform to the discrete-time LTI state-space model (2.1,2.2) and if we assume that the initial condition of the system is $x(0) = 0$, then we obtain the following relation between the input and the output of the system:

$$Y(z) = G(z)U(z)$$

with the transfer function $H(\cdot)$ of the system given by

$$G(z) = C(zI - A)^{-1}B + D = \sum_{k=0}^{\infty} G_k z^{-k} \quad (2.4)$$

Since

$$G(z) = \frac{1}{\det(zI - A)} C \operatorname{adj}(zI - A) B + D,$$

where $\operatorname{adj}(M)$ represents the adjoint matrix of M , the transfer function will always be a rational (matrix) function. If we have a state-space representation of a system, then the transfer function can be computed using (2.4). On the other hand, if we have a SISO transfer function

$$G(z) = \frac{\sum_{i=0}^n a_{n-i} z^i}{\sum_{i=0}^n b_{n-i} z^i}, \quad (2.5)$$

of a discrete-time LTI system with b_0 normalized to 1, then a possible state-space representation is given by the 4-tuple (A, B, C, D) with

$$A = \begin{bmatrix} -b_1 & -b_2 & \cdots & -b_{n-1} & -b_n \\ 1 & 0 & \cdots & 0 & \\ 0 & 1 & \cdots & 0 & \\ \vdots & \vdots & \ddots & \vdots & \vdots \\ 0 & 0 & \cdots & 1 & 0 \end{bmatrix}, B = \begin{bmatrix} 1 \\ 0 \\ \vdots \\ 0 \end{bmatrix},$$

$$C = [a_1 - b_1 a_0 \quad a_2 - b_2 a_0 \quad \cdots \quad a_n - b_n a_0],$$

$$D = a_0.$$

Therefore, several authors have developed methods to transform transfer function matrices into a minimal state-space realization [10, 62]. Since the state-space representation can be converted into a transfer function and vice versa.

2.9 Model reduction

In many area of engineering high-order LTI state-space models are derived and it is desirable if they can be replaced by reduced-order models without incurring too much errors (it is sometimes possible to simply produce satisfactory high order filters and then save it in reduced-order filters implementation, which preserves the key properties of the initial filter of full order ,models of separate components to build the model of a large plant, and so on). Consequently, a wide variety of model reduction methods have been proposed. There are two methods developed of model reduction. These are the theories of balanced realizations and optimal Hankel-norm approximations. With these techniques it is possible to calculate the achievable error between the frequency responses of the full order model and any reduced order model of McMillan degree k . It is also possible to put lower bounds on the same errors [26, 47].

2.10 Identification

Inferring models from observations and studying their properties is really what science is about. The models (“hypotheses,” “laws of nature,” “paradigms,” etc.) may be of more or less formal character, but they have the basic feature that they attempt to link observations together into some pattern. System identification deals with the problem of building mathematical models of dynamical systems based on observed data from the systems. The given data can almost never be explained by a linear model. There are several approaches to generate a linear model of a system. We could, e.g., start from first principles and write down the basic physical laws that govern the behavior of the system. If the resulting model is nonlinear, we could linearize it in the operating point of the system in order to obtain a linear model. This “white-box” approach works for simple examples, but its complexity increases rapidly for real-world systems. An alternative approach is system identification, which is also called the “black-box” approach. In system identification we first collect measurements of the input-output behavior of the system and afterwards we compute a model that explains the measured data. The field of identification has developed rapidly during the past decades. We can now distinguish two main groups of algorithms to identify linear LTI models on the basis of measured data: prediction error methods and subspace methods [6, 43].

2.11 Positive linear systems

Positive systems are, for instance, networks of reservoirs, industrial processes involving chemical reactors, heat exchangers and distillation columns, storage systems (memories, warehouses,...), hierarchical systems, compartmental systems (frequently used when modeling transport and accumulation phenomena of substances in the human bodies), water and atmospheric pollution models, stochastic models where state variables must be nonnegative since they represent probabilities, and many other models commonly used in economy and sociology. One is tempted to assert that positive systems are the most often encountered systems in almost all areas of science and technology, except electro mechanics, where the variables (voltages, currents, forces, positions, velocities) may assume either positive and negative values.

On the other hand, even the simplest electrical circuit, namely, the R - C circuit, is a positive system since the voltage on the capacitor remains non-negative if initially such. Positive linear systems, as any other linear system, satisfy the superposition principle and also a peculiar one, that of comparative dynamics. Such a principle can be expressed by saying that "positive perturbations of inputs, states, and parameters cannot produce a decrease of the state and output at any instant of time following the perturbation". This rule can be quite useful whenever one is interested in abqualitative analysis of the influence of some design parameter (or input) on the system.

DEFINITION 2.1 (externally positive linear system) A linear system (A, b, c^T) is said to be externally positive if and only if its forced output (i.e., the output corresponding to a zero initial state) is nonnegative for every nonnegative input function.

THEOREM 2.1 (condition for external positivity) A linear system is externally positive if and only if its impulse response is nonnegative.

2.12 Max-plus-algebraic models

Max-plus algebra is a class of discrete algebraic systems, also known as an effective tool for modeling and analyzing several types of discrete event systems. In this algebraic system, max and plus operations in conventional algebra are defined as addition and multiplication, respectively. Max-plus algebra are manufacturing systems, telecommunication networks, railway traffic networks, and multi-processor computers. An event corresponds to the start or the end of an activity. For a manufacturing system possible events are: the completion of a part on a machine, a machine breakdown, or a buffer becoming empty. In general, models that describe the behavior of discrete-event systems are nonlinear, but there exists a class of discrete-event systems for which the model becomes linear when formulated in the max-plus algebra, which has maximization (represented by \oplus) and addition (represented as \otimes) as its basic operations. Loosely speaking, this class of discrete-event systems can be characterized as the class of deterministic time-invariant discrete-event systems in which only synchronization and no concurrency occurs. If we write down a model for the behavior of such a system, then the operations maximization and addition arise as follows. Synchronization corresponds to maximization (a new activity can only start

when all the preceding activities have been finished, i.e., after the maximum of the finishing times of the preceding activities), whereas the duration of activities corresponds to addition (the finishing time of an activity is the starting time plus the duration of the activity) [58].

2.13 Linear time-varying models

Time-invariant linear systems no doubt form the most important class of dynamical systems considered in practice and in the literature. It is true that they represent idealizations of the processes encountered in real life. But, even so, the approximations involved are often justified, and design considerations based on linear theory lead to good results in many cases [27]. However, we can also consider time-varying linear systems in which the system matrices also depend on time. Some authors even consider models in which the dimensions of the system matrices may change over time. Minimal state-space realizations for linear time-varying systems can also be characterized as being both controllable and observable [17].

2.14 Nonlinear models

When we use linear models to model physical systems, we are making some assumptions that correspond to an idealization of the real world, which is in fact nonlinear. In analogy with linear systems, some authors define a minimal realization of a nonlinear system as a realization that is both controllable and observable. However, where for a linear systems the dimension of the minimal realization can easily be determined from the input-output data of the system, the situation is far more complicated for nonlinear systems [65, 30] .

2.15 Multi-dimensional minimal state-space realization

In recent years there has been an increasing interest in the study of multi-dimensional systems, due to a wide range of applications in image processing,

seismological data, geophysics, computer tomography, control of multi-pass processes, and so on. An n -dimensional state-space model has the following form:

$$\dot{x} = Ax + bu(\bar{i}), \quad (2.6)$$

$$y(\bar{i}) = cx + du(\bar{i}), \quad (2.7)$$

with

$$\dot{x} = \begin{bmatrix} x_{11}(i_1 + 1, i_2, \dots, i_n) \\ x_{12}(i_1, i_2 + 1, \dots, i_n) \\ \dots \\ x_{1n}(i_1, i_2, \dots, i_n + 1) \\ x_{21}(i_1 + 1, i_2, \dots, i_n) \\ x_{22}(i_1, i_2 + 1, \dots, i_n) \\ \dots \\ x_{2n}(i_1, i_2, \dots, i_n + 1) \\ \dots \\ x_{mn}(i_1, i_2, \dots, i_n + 1) \end{bmatrix}, \quad x = \begin{bmatrix} x_{11}(\bar{i}) \\ x_{12}(\bar{i}) \\ \dots \\ x_{1n}(\bar{i}) \\ x_{21}(\bar{i}) \\ x_{22}(\bar{i}) \\ \dots \\ x_{2n}(\bar{i}) \\ \dots \\ x_{mn}(\bar{i}) \end{bmatrix} \quad (2.8)$$

where $\bar{i} = (i_1, i_2, \dots, i_n)$

The minimal state-space realization problem and the model reduction problem play an important role in the analysis and design of multi-dimensional systems because of the large amount of data involved in multi-dimensional signal processing. However, the general problem of minimal state-space realization of multidimensional systems has not been solved even for two-dimensional systems. Nevertheless, for some special cases minimal state-space realization methods have been derived. However, minimal state-space realizations have been determined for the following special cases as all-pole systems, all-zero systems, systems that can be expanded to continued fraction, systems with separable numerator, systems with separable denominator [69, 45, 3]. At the end of this chapter, we expose an example which discuss the minimal state-space realization in M-D system of a factorable 2-D transfer functions by Antoniou and al [2].

Consider the linear time invariant 2-D system as in figure 2.1 and described

by the spatial transfer function

$$H(z_1, z_2) = \frac{\sum_{i=0}^N \sum_{j=0}^M g_{i,j} z_1^{-i} z_2^{-j}}{\sum_{i=0}^N \sum_{j=0}^M h_{i,j} z_1^{-i} z_2^{-j}}, \quad (2.9)$$

The problem considered is to determine a minimal state-space model of system (2.9) for the following case.

The denominator coefficients of (2.9) can be arbitrary, while the numerator coefficients satisfy the following relationship:

$$g_{i,j} = g_{i,0} g_{0,j} \quad (2.10)$$

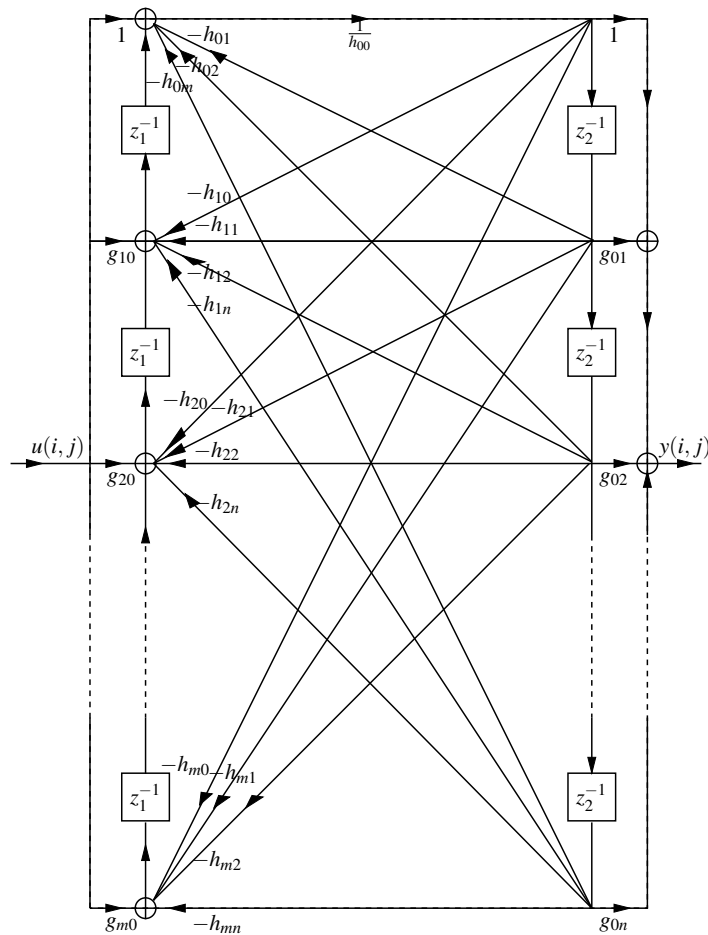


Fig. 2.1 Block diagram of a 2-D transfer function with factorable numerator.

where $g_{i,j}$ assumed, for simplicity, one.

The state-space model sought is of the Givone-Roesser described as follows:

$$\begin{bmatrix} x^h(n_1+1, n_2) \\ x^v(n_1, n_2+1) \end{bmatrix} = \begin{bmatrix} A_1 & A_2 \\ A_3 & A_4 \end{bmatrix} \begin{bmatrix} x^h(n_1, n_2) \\ x^v(n_1, n_2) \end{bmatrix} + \begin{bmatrix} B_1 \\ B_2 \end{bmatrix} u(n_1, n_2), \quad (2.11)$$

$$y(n_1, n_2) = \begin{bmatrix} C_1 & C_2 \end{bmatrix} \begin{bmatrix} x^h(n_1, n_2) \\ x^v(n_1, n_2) \end{bmatrix} + Du(n_1, n_2), \quad (2.12)$$

where $x^h(n_1, n_2) \in \mathbb{R}^{n_h}$ and $x^v(n_1, n_2) \in \mathbb{R}^{n_v}$, $u(i, j) \in \mathbb{R}_1$ is the input vector, and $y(i, j) \in \mathbb{R}_1$ is the output vector. A 2-D minimal state-space realization having the form (2.11, 2.12) where

$$A_1 = \begin{bmatrix} -\frac{h_{10}}{h_{00}} & 1 & 0 & \cdots & 0 \\ \cdot & 0 & \ddots & \ddots & \cdot \\ \vdots & \vdots & \ddots & \ddots & \vdots \\ \cdot & \cdot & \ddots & \ddots & 0 \\ \cdot & 0 & & \ddots & 1 \\ -\frac{h_{m0}}{h_{00}} & 0 & \cdot & \cdots & 0 \end{bmatrix},$$

$$A_2 = \begin{bmatrix} \frac{h_{10}h_{01}}{h_{00}} - h_{11} & \cdots & \frac{h_{10}h_{0n}}{h_{00}} - h_{1n} \\ \vdots & \vdots & \vdots \\ \frac{h_{m0}h_{01}}{h_{00}} - h_{m1} & \cdots & \frac{h_{m0}h_{0n}}{h_{00}} - h_{mn} \end{bmatrix},$$

$$A_3 = \begin{bmatrix} -\frac{1}{h_{00}} & 0 & \cdots & \cdots & 0 \\ 0 & 0 & \ddots & & \cdot \\ \vdots & \ddots & \ddots & \ddots & \vdots \\ \cdot & \cdot & \ddots & \ddots & 0 \\ \cdot & 0 & & \ddots & 0 \\ 0 & \cdots & \cdots & 0 & 0 \end{bmatrix},$$

$$A_4 = \begin{bmatrix} -\frac{h_{01}}{h_{00}} & \cdots & \cdots & \cdot & \cdot & -\frac{h_{0n}}{h_{00}} \\ 1 & 0 & \cdots & \cdot & & 0 \\ 0 & \ddots & \ddots & & & \cdot \\ \vdots & \ddots & \ddots & \ddots & \ddots & \vdots \\ 0 & \cdots & \cdots & 0 & 1 & 0 \end{bmatrix},$$

$$\begin{aligned}
 b_1 &= \begin{bmatrix} g_{10} - \frac{h_{10}}{h_{00}} \\ \vdots \\ g_{m0} - \frac{h_{m0}}{h_{00}} \end{bmatrix}, \\
 b_2 &= \begin{bmatrix} \frac{1}{h_{00}} \\ \vdots \\ 0 \end{bmatrix}, \\
 c_1 &= \left[\frac{1}{h_{00}} \quad 0 \quad \cdots \quad 0 \right], \\
 c_2 &= \left[g_{01} - \frac{h_{01}}{h_{00}} \quad \cdots \quad g_{0n} - \frac{h_{0n}}{h_{00}} \right], \\
 D &= \frac{1}{h_{00}}.
 \end{aligned}$$

See Appendix C

2.16 Conclusion

In this chapter, we have cited some problem of realizing minimal state space. The most of problem has been satisfactorily solved. But the research has been renewed in various fields such as reduction, approximation and pattern identification. In particular, for general nonlinear systems and multidimensional systems, there is still a lot of active research going on.

Chapter 3

Minimal state-space realizations of proposed structures in lattice and ladder-lattice form

3.1 Introduction

Realizing a system with a multidimensional state space model having minimal dimensionality is a significant and non-trivial problem. The need to provide minimal realization arises out of several requirements [45, 22]. To begin with, in general, non-minimal realizations often cause theoretical and/or computational difficulties. In the N-D systems area, the problem of constructing state-space realizations is of fundamental importance. Also, it is important to keep in mind that the amount of data handled by 2-D or more systems is often very large. Thus, there are pressing needs to reduce the hardware requirements as much as possible. Furthermore, various problems such as round-off error analysis, coefficient sensitivity, optimization, etc., can be studied much more effectively using the state space approach. These reasons, among others, conspire to characterize the task of minimal realization as one of great utility. The problem of transforming a transfer function into a differential equation (a state-space form) is important in system theory and because of the inherent absence of the non-applicability of the fundamental theorem of algebra to multidimensional polynomials. Example, we cannot factored multi-variable polynomials in general (Appendix D) then, we have a crucial problem for multidimensional filters and

systems. So, we require to have multidimensional systems with a minimal delay elements. This requirement can be explained not only by the hardware specifications, but also gives no advantage and may cause numerical difficulties. Since the general problem of minimal state-space realization of multidimensional systems has not been solved even for two-dimensional systems. Nevertheless, for some special cases, like all-pole filters, discrete time lossless bounded real functions, separable and factorable systems and lattice filters [16, 3, 37, 69, 5, 4], etc.

3.2 Proposed lattice structure and realization

The lattice-ladder realization is the most important among the circuit structures proposed for implementation of digital filters, because of its robustness and modularity, and has many applications in digital filtering and adaptive signal processing. We propose a new lattice-ladder structure of 2-D discrete filter, composed of a delay unit z_1^{-1} and a basic lattice section $z_1 z_2^{-1}$. Using a matrix representation of the elementary lattice sections, we derived a 2-D transfer functions of the generalized circuit. The generalized realization with the minimal delay elements utilizes the minimal number of basic lattice sections. Besides, the state space equations for the 2-D digital filter are presented where the dimension of the matrix-vectors of the proposed ladder-lattice verifies the minimal state space realization.

3.2.1 Proposed ladder lattice 2-d digital filter

Figure 3.1 shows the proposed lattice-ladder structure for constructing a discrete 2-D filter. This structure has two basic lattice sections z_1^{-1} and $z_1 z_2^{-1}$. The input-output relationship of the proposed lattice structure shown in figure 3.1 is given by the following matrix representation

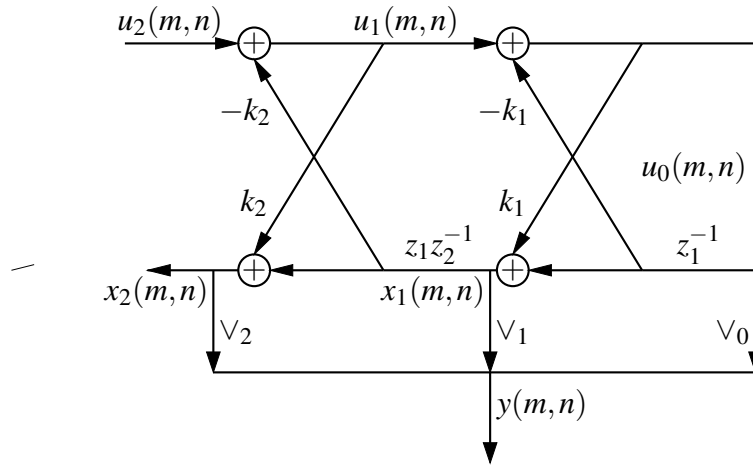


Fig. 3.1 The proposed lattice- ladder 2-D digital filter with two basic lattice sections.

$$\begin{bmatrix} X_2(z_1, z_2) \\ U_2(z_1, z_2) \end{bmatrix} = \begin{bmatrix} 1 & k_2 z_1 z_2^{-1} \\ k_2 & z_1 z_2^{-1} \end{bmatrix} \begin{bmatrix} 1 & k_1 z_1^{-1} \\ k_1 & z_1^{-1} \end{bmatrix} U_0(z_1, z_2) \quad (3.1)$$

$$Y(z_1, z_2) = X_2(z_1, z_2) V_2 + X_1(z_1, z_2) V_1 + X_0(z_1, z_2) V_0 \quad (3.2)$$

$$U_0(z_1, z_2) = X_0(z_1, z_2) \quad (3.3)$$

From ((3.1),(3.2),(3.3)) and after rearrangement, one can construct the transfer function of a 2-D recursive digital filter with order 1×1 as follows

$$H_2(z_1, z_2) = \frac{Y(z_1, z_2)}{U_2(z_1, z_2)}$$

Thus,

$$H_2(z_1, z_2) = \frac{V_0 + V_1 k_1 + V_2 k_2 + (V_1 + V_2 k_1 k_2) z_1^{-1} + V_2 z_2^{-1} + V_2 k_1 z_1 z_2^{-1}}{1 + k_1 z_1^{-1} + k_2 z_2^{-1} + k_1 k_2 z_1 z_2^{-1}} \quad (3.4)$$

3.2.2 Realization

To generalize the structure lattice-ladder of figure 3.1 with two basic lattice sections z_1^{-1} and $z_1 z_2^{-1}$, we should cascade $N z_1^{-1}$ and $M z_1 z_2^{-1}$ delay units

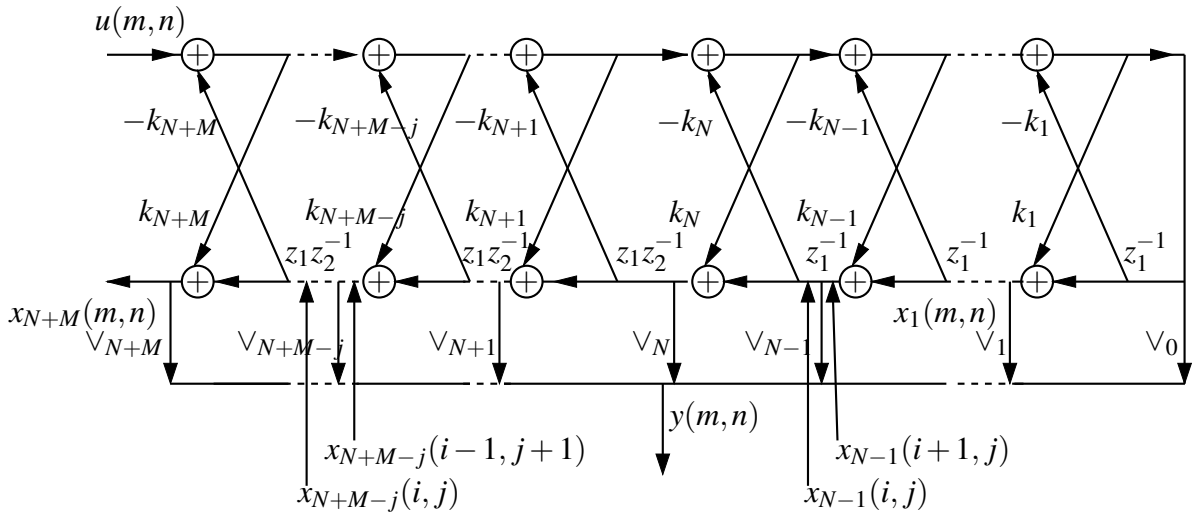


Fig. 3.2 The proposed lattice- ladder 2-D digital filter with $N \times M$ basic lattice sections.

as depicted in figure 3.2. Thus, the generalized lattice realization can be transformed into the following 2-D state-space model

$$\begin{aligned} \dot{x}(i, j) &= Ax(i, j) + bu(i, j), \\ y(i, j) &= cx(i, j) + du(i, j), \end{aligned} \quad (3.5)$$

where

$$x(i, j) = \begin{bmatrix} x_{M+N}(i, j) \\ x_{M+N-1}(i, j) \\ \dots \\ x_{N+1}(i, j) \\ x_N(i, j) \\ \dots \\ x_1(i, j) \end{bmatrix}, \quad \dot{x}(i, j) = \begin{bmatrix} x_{M+N}(i-1, j+1) \\ x_{M+N-1}(i-1, j+1) \\ \dots \\ x_{N+1}(i-1, j+1) \\ x_N(i+1, j) \\ \dots \\ x_1(i+1, j) \end{bmatrix} \quad (3.6)$$

where $u(i, j)$, $y(i, j)$ and $x(i, j)$ are the input, the output and the state, respectively, and A is the state transition matrix. The dimensions of the matrix-vectors A , b and c are $(M+N) \times (M+N)$, $(M+N) \times 1$ and $1 \times (M+N)$, respectively. The minimal state space model is to transform a transfer function matrices into a minimal state space realization and vice versa the state space representation can be converted into a transfer function. It can be

shown that the proposed circuit block diagram in figure 3.2 composed of (M+N) elementary lattice sections generate the minimal dimensions of the matrices A, b, and c. Applying the 2-D z-transform on (3.6), we obtain the transfer function which takes the following form

$$H_{M+N}(z_1, z_2) = \frac{Y(z_1, z_2)}{U_{M+N}(z_1, z_2)} = d + c(Z - A)^{-1}b. \quad (3.7)$$

where

$$Z = z_2 z_1^{-1} I_{M+N} \oplus \dots z_2 z_1^{-1} I_{M+N} \oplus z_1 I_{M+N} \oplus \dots z_1 I_{M+N}$$

with \oplus denoting the direct sum.

3.2.3 State space realization

The new 2-D ladder-lattice circuit is generated as depicted in the figure 3.2, and in order to derive the state-space model (3.6). First, label the outputs of the delay elements that correspond to the states of the model. Next, write by inspection one-state equation for every delay element and then, rearrange the equations to have blocks of every state variables. Finally generalize the results. We can conclude that the matrix-vectors A, b, c, and the scalar d of the state space model, are derived. The new 2-D structure has a minimal number of basics lattice section elements z_1^{-1} and $z_1 z_2^{-1}$. It is noted that the cascaded circuit implementation with the minimal delay elements utilizes the minimal number of basic lattice sections (M+N). The matrices A, b, c, and the scalar d of the derived 2-D state space model Roesser type [56] have the following form

$$A = \begin{bmatrix} -k_{M+N-1}k_{M+N} & 1 - k_{M+N-1}^2 & \dots & 0 & 0 & 0 \\ -k_{M+N-2}k_{M+N} & -k_{M+N-2}k_{M+N-1} & 1 - k_{M+N-2}^2 & \dots & \dots & 0 \\ \vdots & \dots & \dots & \dots & \vdots & \vdots \\ \vdots & \vdots & \ddots & \ddots & \vdots & \vdots \\ -k_1 k_{M+N} & \vdots & \ddots & \ddots & -k_1 k_2 & 1 - k_1^2 \\ -k_{M+N} & -k_{M+N-1} & \dots & \dots & -k_2 & -k_1 \end{bmatrix},$$

$$b = [k_{M+N-1} \quad k_{M+N-2} \quad 0 \quad \dots \quad k_1 \quad 1]^T,$$

$$c = [c_1 \quad c_2 \quad \dots \quad \dots \quad c_{M+N-1} \quad c_{M+N}],$$

$$c_j = (1 - k_{M+N-L}^2) \vee_{M+N-L} - \sum_{i=1}^{M+N-j} k_i k_{M+N-L} \vee_i - k_{M+N-L} \vee_0, \quad j = 1, \dots, N+M-2, \quad L = j-1,$$

$$c_{M+N-1} = (1 - k_2^2) \vee_2 - k_1 k_2 \vee_1 - k_2 \vee_0,$$

$$c_{M+N} = (1 - k_1^2) \vee_1 - k_1 \vee_0,$$

$$d = \sum_{i=1}^{M+N} k_i \vee_i + \vee_0. \tag{3.8}$$

It is noted that the dimension of the state space $x(i,j)$ is $1 \times (N+M)$ and the matrix A has minimal dimension $(N+M) \times (N+M)$, resulting from the corresponding minimal circuit realization.

$k_i, i = 1, \dots, N+M.$ are reflection coefficients.

$\vee_i, i = 1, \dots, N+M.$ are ladder network.

3.2.4 Example

First order 2-D ladder-lattice digital filter

For simplicity consider the first order 2-D ladder-lattice filter, by substituting $N=M=1$ into (3.6) and (3.8). In this case, the corresponding state space realization takes the form

$$\begin{aligned} \dot{x}(i, j) &= Ax(i, j) + bu(i, j), \\ y(i, j) &= cx(i, j) + du(i, j), \end{aligned}$$

where

$$x(i, j) = \begin{bmatrix} x_2(i, j) \\ x_1(i, j) \end{bmatrix}, \quad \dot{x}(i, j) = \begin{bmatrix} x_2(i-1, j+1) \\ x_1(i+1, j) \end{bmatrix} \tag{3.9}$$

The matrix A , the vectors b, c and the scalar d have the following quadruple state-space form

$$\left[\begin{array}{cc|c} \begin{bmatrix} -k_1 k_2 & 1 - k_1^2 \\ -k_2 & -k_1 \end{bmatrix} & \begin{bmatrix} k_1 \\ 1 \end{bmatrix} \\ \hline \begin{bmatrix} (1 - k_2^2) \vee_2 - k_1 k_2 \vee_1 - k_2 \vee_0 & (1 - k_1^2) \vee_1 - k_1 \vee_0 \end{bmatrix} & \vee_0 + k_1 \vee_1 + k_2 \vee_2 \end{array} \right] \tag{3.10}$$

The dimension of the state space $x(i,j)$ is 1×2 , the number of basics lattice section elements, namely z_1^{-1} and $z_1 z_2^{-1}$ are 2. The dimensions of the matrix-vectors A , b , c are 2×2 , 2×1 , 1×2 , respectively. The state space is minimal. The 2-D transfer function of the state space by using (3.7) is

$$H(z_1, z_2) = v_0 + k_1 v_1 + k_2 v_2 + \left[(1 - k_2)^2 v_2 - k_1 k_2 v_1 - k_2 v_0 \quad (1 - k_1)^2 v_1 - k_1 v_0 \right] \cdot \left[\begin{bmatrix} z_2 z_1^{-1} & 0 \\ 0 & z_1 \end{bmatrix} - \begin{bmatrix} -k_1 k_2 & 1 - k_1^2 \\ -k_2 & -k_1 \end{bmatrix} \right]^{-1} \begin{bmatrix} k_1 \\ 1 \end{bmatrix},$$

$$H_2(z_1, z_2) = \frac{v_0 + v_1 k_1 + v_2 k_2 + (v_1 + v_2 k_1 k_2) z_1^{-1} + v_2 z_2^{-1} + v_2 k_1 z_1 z_2^{-1}}{1 + k_1 z_1^{-1} + k_2 z_2^{-1} + k_1 k_2 z_1 z_2^{-1}}. \quad (3.11)$$

We can see that the transfer function (3.11) is the same as (3.4).

For $v_2 = 1$ and $v_1 = v_0 = 0$. The above transfer function (3.4) takes the form

$$H_2(z_1, z_2) = \frac{k_2 + k_1 k_2 z_1^{-1} + z_2^{-1} + k_1 z_1 z_2^{-1}}{1 + k_1 z_1^{-1} + k_2 z_2^{-1} + k_1 k_2 z_1 z_2^{-1}} \quad (3.12)$$

It is obvious that the above transfer function (3.12) can provide filters having all-pass and all-pole characteristics as in [40].

$$H_2(z_1, z_2) = z_2^{-1} \frac{D_2(z_1^{-1}, z_2^{-1})}{D_2(z_1, z_2)}$$

Notice in particular that, for the ladder network $v_{M+N} = 1$ and $v_i = 0$, $i = 0, 1, \dots, M+N-1$, we find the proposed structure in [40].

2-D ladder-lattice filter with order 2×1

In this example we consider a low dimension filter $N = 2$ and $M = 1$, the 2×1 2-D ladder-lattice filter is shown in figure 3.3, the corresponding state space realization takes the form,

$$x(i, j) = \begin{bmatrix} x_3(i, j) \\ x_2(i, j) \\ x_1(i, j) \end{bmatrix}, \quad \dot{x}(i, j) = \begin{bmatrix} x_3(i-1, j+1) \\ x_2(i+1, j) \\ x_1(i+1, j) \end{bmatrix} \quad (3.13)$$

3.4 Proposed 3-D Lattice Structure

In this section we propose a new lattice structure of 3-D digital filter as in figure 4.11, composed of two delay units z_1^{-1} , z_2^{-1} and basic lattice section $z_1 z_3^{-1}$. From this structure and using a matrix representation of the basic lattice sections, we derived transfer functions of the proposed 3-D digital lattice filters, 3-D FIR, and 3-D all-pass filters. The proposed structure is composed by a minimal number of delays and a minimal number of basic lattice sections. Furthermore, we have considered the description of the proposed lattice structure by using a state-space n-D ($n > 2$) Roesser form description presented in [25]. and the implementations suggested by the authors in [40, 5, 39] Besides, the state space equations for 3-D digital filter are presented where the dimension of the matrices of the proposed lattice structure verify the minimal state space realization. With the characteristics of unit magnitude and prescribed phase, specifications can be preserved at all frequencies. These properties enable all-pass filters to play a vital role in various signal processing applications [36, 20, 40].

3.4.1 Proposed FIR Lattice Structure

We propose a lattice structure with two delay units z_1^{-1} , z_2^{-1} and basic lattice section $z_1 z_3^{-1}$ to constructing a first order 3-D Finite Impulse Response (FIR) digital filter illustrated in figure 3.4. The 3-D forward transfer function can be computed using the following matrix:

$$\begin{bmatrix} Y(z_1, z_2, z_3) \\ U_3(z_1, z_2, z_3) \end{bmatrix} = \begin{bmatrix} 1 & k_2 z_1 z_3^{-1} \\ k_2 & z_1 z_3^{-1} \end{bmatrix} \begin{bmatrix} 1 & k_1 z_2^{-1} \\ k_1 & z_2^{-1} \end{bmatrix} \begin{bmatrix} 1 & k_0 z_1^{-1} \\ k_0 & z_1^{-1} \end{bmatrix} X_3(z_1, z_2, z_3) \quad (3.15)$$

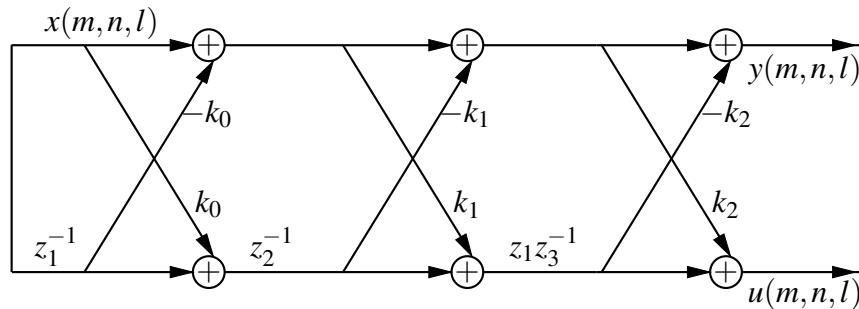


Fig. 3.4 3-D first order FIR lattice structure.

From (3.15), one can get the expressions of the transfer function of a 3-D FIR digital filter in the order $1 \times 1 \times 1$ is given by

$$T(z_1, z_2, z_3) = \frac{Y(z_1, z_2, z_3)}{X(z_1, z_2, z_3)} \quad (3.16)$$

where

$$T(z_1, z_2, z_3) = 1 + k_0 k_1 z_2^{-1} + k_0 z_1^{-1} + k_1 z_1^{-1} z_2^{-1} + k_1 k_2 z_1 z_3^{-1} + k_0 k_2 z_1 z_2^{-1} z_3^{-1} + k_2 z_2^{-1} z_3^{-1} + k_0 k_1 k_2 z_3^{-1} \quad (3.17)$$

3.4.2 Proposed Recursive Lattice Structure

Based on the above 3-D FIR lattice structures in figure 3.4. We propose a 3-D lattice structure with three basic lattice sections for constructing a 3-D recursive digital filter figure 3.5. From figure 3.5, we have the following matrix representations

$$\begin{bmatrix} X_3(z_1, z_2, z_3) \\ U_3(z_1, z_2, z_3) \end{bmatrix} = \begin{bmatrix} 1 & k_2 z_1 z_3^{-1} \\ k_2 & z_1 z_3^{-1} \end{bmatrix} \begin{bmatrix} 1 & k_1 z_2^{-1} \\ k_1 & z_2^{-1} \end{bmatrix} \begin{bmatrix} 1 & k_0 z_1^{-1} \\ k_0 & z_1^{-1} \end{bmatrix} Y(z_1, z_2, z_3) \quad (3.17)$$

From (??), one can get the expressions

$$X_3(z_1, z_2, z_3) = T(z_1, z_2, z_3) Y(z_1, z_2, z_3) \quad (3.18)$$

$$U_3(z_1, z_2, z_3) = S(z_1, z_2, z_3) Y(z_1, z_2, z_3) \quad (3.19)$$

where

$$T(z_1, z_2, z_3) = 1 + k_0 k_1 z_2^{-1} + k_0 z_1^{-1} + k_1 z_1^{-1} z_2^{-1} + k_1 k_2 z_1 z_3^{-1} + k_0 k_2 z_1 z_2^{-1} z_3^{-1} + k_2 z_2^{-1} z_3^{-1} + k_0 k_1 k_2 z_3^{-1} \quad (3.20)$$

$$S(z_1, z_2, z_3) = k_2 + k_2 k_0 k_1 z_1 z_2^{-1} + k_1 z_2 z_3^{-1} + k_0 z_1 z_3^{-1} + k_2 k_0 z_1^{-1} + k_2 k_1 z_2^{-1} + k_0 z_2 z_3^{-1} z_1^{-1} + z_3^{-1} \quad (3.21)$$

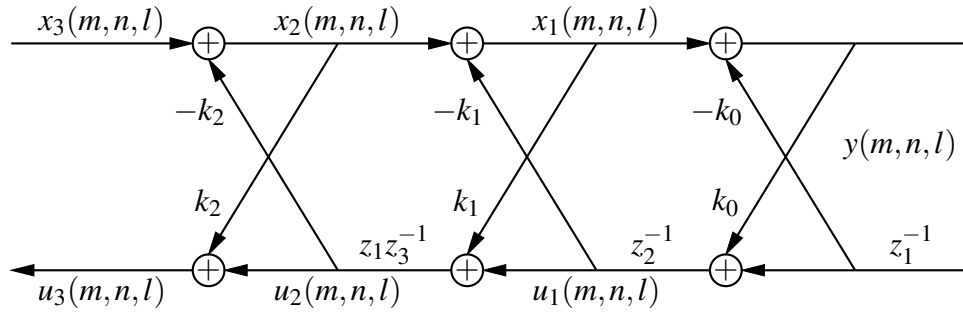


Fig. 3.5 The proposed 3-D recursive lattice structure.

Based on (3.18), we obtain the transfer function of a 3-D digital all-pole filter

$$\frac{Y(z_1, z_2, z_3)}{X_3(z_1, z_2, z_3)} = \frac{1}{T(z_1, z_2, z_3)}$$

After rearrangement, one can get the following relationship

$$S(z_1, z_2, z_3) = z_2^{-1} z_3^{-1} T(z_1^{-1}, z_2^{-1}, z_3^{-1}) \quad (3.23)$$

From (3.18), (3.19) and (3.23), one can construct the forward transfer function of 3-D recursive digital all-pass filter of order $1 \times 1 \times 1$ as follows

$$H_A(z_1, z_2, z_3) = \frac{U_3(z_1, z_2, z_3)}{X_3(z_1, z_2, z_3)} = z_2^{-1} z_3^{-1} \frac{T(z_1^{-1}, z_2^{-1}, z_3^{-1})}{T(z_1, z_2, z_3)} \quad (3.24)$$

It should be noted that the numerator and denominator polynomials of $H_A(z_1, z_2, z_3)$ are mirror images of each other, which is a general property of all-pass system [54].

3.4.3 State Space Realization

To construct a general 3-D recursive digital all-pass filter with order $N \times N \times N$, we generalize the structure of figure 3.5 by cascading $N z_1^{-1}$, $N z_2^{-1}$ delay units and $N z_1 z_3^{-1}$ basics lattice section as shown in figure 3.6. The related state space 3-D model have the following structure

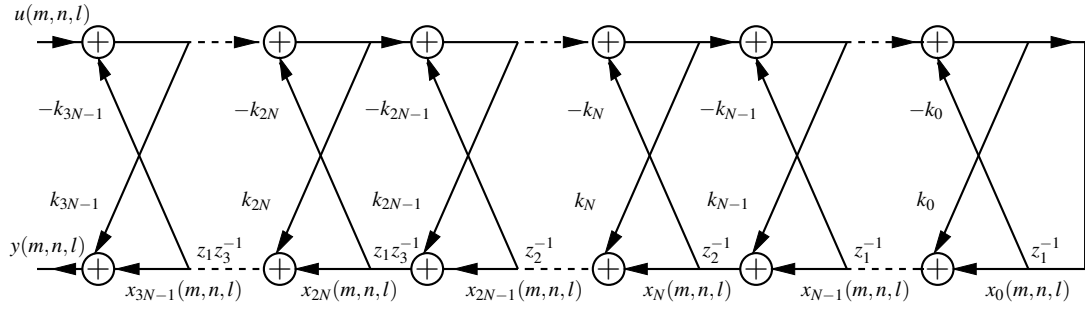


Fig. 3.6 The proposed generalized 3-D recursive digital all-pass filter with order $N \times N \times N$.

$$\begin{aligned} \dot{x}(i, j, l) &= Ax(i, j, l) + bu(i, j, l), \\ y(i, j, l) &= cx(i, j, l) + du(i, j, l), \end{aligned} \quad (3.25)$$

where:

$$x(i, j, l) = \begin{bmatrix} x_{3N-1}(i, j, l) \\ x_{3N-2}(i, j, l) \\ \dots \\ x_{2N}(i, j, l) \\ x_{2N-1}(i, j, l) \\ \dots \\ x_N(i, j, l) \\ \dots \\ x_{N-1}(i, j, l) \\ \dots \\ x_0(i, j, l) \end{bmatrix}, \quad \dot{x}(i, j, l) = \begin{bmatrix} x_{3N-1}(i-1, j, l+1) \\ x_{3N-2}(i-1, j, l+1) \\ \dots \\ x_{2N}(i-1, j, l+1) \\ x_{2N-1}(i, j+1, l) \\ \dots \\ x_N(i, j+1, l) \\ \dots \\ x_{N-1}(i+1, j, l) \\ \dots \\ x_0(i+1, j, l) \end{bmatrix}$$

and $u(i, j, l)$, $y(i, j, l)$ is respectively the input and the output, A is the transition matrix. A , b , c , and d are given by

$$\mathbf{A} = \begin{bmatrix} -k_{3N-1}k_{3N-2} & k_{3N-1}k_{3N-3} & \dots & \dots & k_{3N-1}k_0 & -k_{3N-1} \\ k_{3N-2}^2 - 1 & -k_{3N-2}k_{3N-3} & \dots & \dots & -k_{3N-2}k_0 & k_{3N-2} \\ 0 & k_{3N-3}^2 - 1 & \dots & \dots & k_{3N-3}k_0 & -k_{3N-3} \\ 0 & 0 & \ddots & \ddots & \vdots & \vdots \\ \vdots & \vdots & \ddots & \ddots & \vdots & \vdots \\ 0 & \dots & \dots & 0 & k_0^2 - 1 & -k_0 \end{bmatrix},$$

$$\begin{aligned}
\mathbf{b} &= \left[k_{3N-2} \quad (1 - k_{3N-2}^2)/k_{3N-1} \quad 0 \quad \dots \quad \dots \quad 0 \right]^T, & k_{3N-1} &\neq 0, \\
\mathbf{c} &= \left[1 - k_{3N-1}^2 \quad 0 \quad \dots \quad \dots \quad 0 \right], \\
\mathbf{d} &= k_{3N-1}.
\end{aligned} \tag{3.26}$$

The matrices A , b and c of the above 3-D state space model, having the following dimensions respectively: $3N \times 3N$, $3N \times 1$ and $1 \times 3N$. It is noted that the generalized circuit and state space realizations of the proposed lattice structure composed of $3N$ basic lattice sections produces the minimal dimensions of the matrices A , b and c .

Applying the z -transform for both sides of (3.25), we obtain the 3-D transfer function which takes the following form:

$$H(z_1, z_2, z_3) = \frac{Y(z_1, z_2, z_3)}{U(z_1, z_2, z_3)} = d + c(Z - A)^{-1}b. \tag{3.27}$$

where

$$Z = z_3 z_1^{-1} I_n \oplus \dots \oplus z_3 z_1^{-1} I_n \oplus z_2 I_n \oplus \dots \oplus z_2 I_n \oplus z_1 I_n \oplus \dots \oplus z_1 I_n$$

with \oplus denoting the direct sum.

We can obtain the transfer function $H_A(z_1, z_2, z_3)$ of (3.24) from (3.27) by substituting $N = 1$ into (3.26) and (3.27)

$$\begin{aligned}
H_A(z_1, z_2, z_3) &= k_2 + \begin{bmatrix} 1 - k_2^2 & 0 & 0 \end{bmatrix} \left[\begin{bmatrix} z_3 z_1^{-1} & 0 & 0 \\ 0 & z_2 & 0 \\ 0 & 0 & z_1 \end{bmatrix} - \begin{bmatrix} -k_2 k_1 & k_2 k_0 & -k_2 \\ k_1^2 - 1 & -k_1 k_0 & k_1 \\ 0 & k_0^2 - 1 & -k_0 \end{bmatrix} \right]^{-1} \begin{bmatrix} k_1 \\ (1 - k_1^2)/k_2 \\ 0 \end{bmatrix}, \\
H_A(z_1, z_2, z_3) &= z_2^{-1} z_3^{-1} \frac{T(z_1^{-1}, z_2^{-1}, z_3^{-1})}{T(z_1, z_2, z_3)}.
\end{aligned} \tag{3.28}$$

3.4.4 Interpretation

In this section, we have proposed a new lattice structure of a 3-D digital filter, we calculate the transfer function by using the matrix representations. 3-D all pass lattice filters can be constructed. It is noted the transfer function all pass lattice digital filter derived has the mirror-image symmetry relation between the numerator and denominator polynomials as in the all-pass

systems. We calculate the state-space realizations of a 3-D lattice all pass digital structured filter and using the Roesser 3-D state-space model to verify the characteristics of the constructed 3-D recursive digital lattice filter. This circuit configuration is characterized by a minimal realization.

Chapter 4

Application of the proposed realization two and Three-Dimensional IIR Notch Filter Design:simulation and interpretation

4.1 Introduction

Multidimensional digital filters have maintained tremendous vitality over the last three decades for numerous applications in diverse areas such as image processing, geophysics, radar, bio-medical engineering, digital control systems and many more. Digital filters are mainly used to change the characteristics of an input digital signal into an output digital signal with desirable properties. Two classes of digital filters can be distinguished: infinite-impulse response (IIR) or finite-impulse response (FIR) with recursive or non-recursive operations. Digital notch filters have the property of removing a single non-desired frequency component or a narrow band sinusoidal interference from an input signal. Notch filters can be FIR or IIR filters. The latter are preferred in practice when transition zone bandwidth is very narrow because it requires less arithmetic operations compared to FIR notch filter. Different approaches are proposed for the design of IIR notch filters. One of these approaches uses all pass filters, which is considered as an

effective analytic method. However, to eliminate unknown or time-varying narrow-band components from observed time series, it is preferred to use adaptive notch filter. There are other techniques based on: wavelet transform and statistical curve fitting and feedback structure. The purpose of this chapter is to present a design procedure for 2-D and 3-D IIR notch filter.

4.2 Notch filter characteristics

In signal processing, a band-stop filter or band-rejection filter known also as a notch filter, blocks and rejects frequencies that lie between its two cut-off frequency points passes all those frequencies either side of this range. It is the opposite of a band-pass filter. A notch filter is a band-stop filter with a very narrow stopband. The amplitude response $\|H(e^{j\omega})\|$ of a typical notch filter designated as shown in figure 4.1, characterized by the notch frequency ω_n , and 3-dB rejection bandwidth BW. For an ideal notch filter, BW should be zero, the passband magnitude should be unity (zero dB) everywhere either side of the notch and the attenuation at the notch frequency should be infinite. Unfortunately, the ideal notch filter is not physically realizable and must be approximated in practice. The important characteristics of a notch filter are:

- a. The amount of insertion loss in its pass region.
- b. The flatness of the amplitude response in the bandpass region.
- c. The depth of the rejection notch.
- d. The width of the rejection notch at its ultimate rejection level.
- e. The width of the rejection notch measured down from the band pass region of the notch.

Typically it is desired to have the lowest possible loss and no ripple in the pass region, as much depth at the ultimate point in the notch as possible, good width at the bottom of the notch and very narrow width at the 3-db points on the notch.

4.3 Applications of notch filters

Notch filter circuits are widely used in television receivers in the IF section to eliminate discrete frequency regions where unwanted carriers appear from adjacent channels. Notch filters are also used widely in cable television

systems to deny access to certain signals or alternatively to remove interference in other signals. Also notch filters are used at different technologies as follows

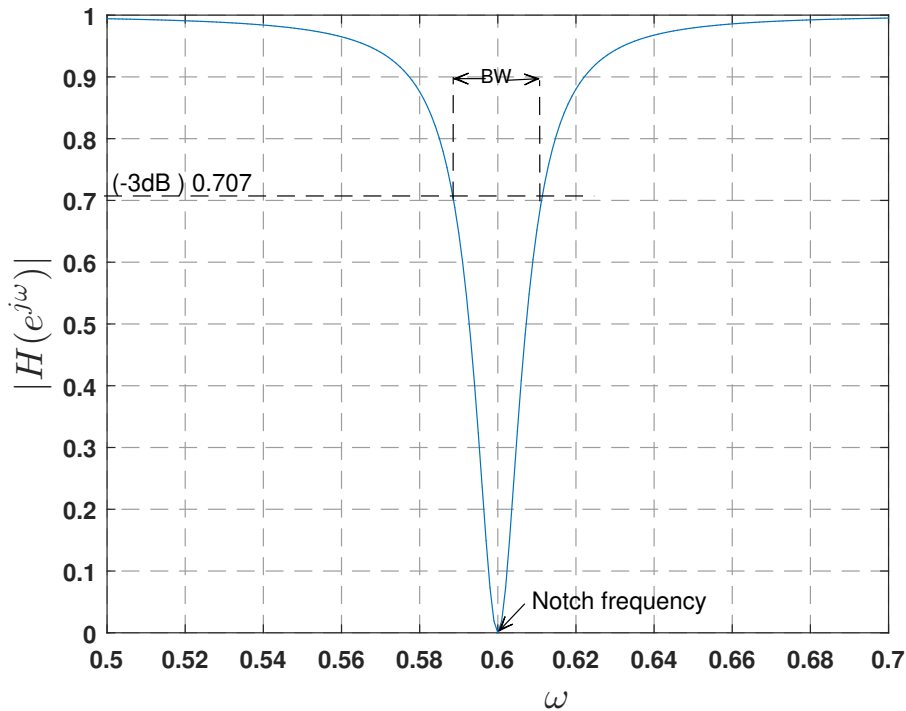


Fig. 4.1 The magnitude response of 1D notch filter $\|H(e^{j\omega})\|$.

1. In signal and image processing Notch filters are highly preferred to remove the contamination on an image and reject noise.
2. Notch filter are used as noise reducers in (telephone line and DSL internet services)
3. Notch filters are generally used to cancel 50/60 Hz power line interference in the recording of electrocardiograms (ECGs).
4. Notch filters help to remove the interference on the line which will reduce the DSL performance.
5. These are used in music and some acoustic applications.
6. Notch filters are used to eliminate the unwanted harmonics in communication electronics .

7. These are used to reduce the static on radio, which are commonly used in our daily life.
8. These are used to reduce blocking artifact from DCT coded image .

4.4 Digital notch filter design techniques

A notch filter is a device which is generally presumed to pass all frequencies except for a very narrow band which is 'notched out'. This type of filter is sometimes called a band elimination filter as well. In practice, the notch filter may have only a limited band for passing signals but typically this band width is several octaves wide. Digital Notch filters may be designed as finite impulse response (FIR) or infinite impulse response (IIR) structures by using standard design techniques. A number of design approaches are available in the literature for IIR as well as for FIR filters [52, 75, 70, 32]. These FIR and IIR digital notch filters have their own specific features. Based upon the requirements for the specific application one of the above digital filter is chosen. The IIR notch filters are preferred in practice when transition zone bandwidth is very narrow because it requires less arithmetic operations compared to FIR notch filter. It can be designed for lower orders to approximate a given set of specifications designs. This implies that the signal processing by IIR filters is faster than that by the FIR ones. However, the implementation complexity of an FIR filter is not of much concern as tremendous advancement in DSP has taken place due to FFT techniques and field programmable gate array (FPGA) technology. The major problems with IIR filters are that they are essentially unstable and can not provide linear phase response. There are different approaches proposed for the design of IIR notch filters.

1. Approaches uses all pass filters, which is considered as an effective analytic method [49, 64] and exhibits low sensitivity to coefficient quantization and allows standard low-pass, high-pass and band-pass (band-stop) filters to be realized as well as with arbitrary number of bands. Such approach can be modified and applied on design of IIR notch filters.

2. Approaches transforming an analog notch filter into digital IIR filter. However this method preserve only magnitude characteristic and it is not convenient for transformation of analogue filters with linear phase.
3. Approach is pole-zero placements in the z plane [49] with effort to control size of the pass-band width and to solve problem of asymmetric pass-band boundaries according to notch frequency position.
4. Adaptive notch filter are used to eliminate unknown or slowly time-varying narrow-band components from observed time series (Digital linear phase notch filter design based on IIR all-pass filter application) [35].
5. There are other techniques based on: wavelet transform and statistical curve fitting [31] and feedback structure [48]

4.5 Notch filter based on all-pass filter

The authors in [54] have developed an interesting design approach of a notch filter based on all-pass filter. The all-pass filter is implemented in a lattice structure, consider the all-pass lattice topology shown in figure 4.2. It has the all-pass transfer function

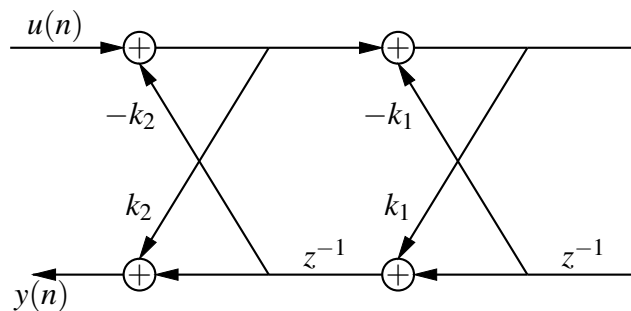


Fig. 4.2 Lattice second-order all-pass filter.

$$A(z) = \frac{Y(z)}{U(z)} = \frac{k_2 + k_1(1 + k_2)z^{-1} + z^{-2}}{1 + k_1(1 + k_2)z^{-1} + k_2z^{-2}}. \quad (4.1)$$

$$H_n(z) = \frac{1 + A(z)}{2} \quad (4.2)$$

$$H_r(z) = \frac{1 - A(z)}{2} \tag{4.3}$$

We can derive (4.2) and (4.3) from (4.1) this means that we can construct notch and perfect resonant filters from an all-pass filter [15] as in figure 4.3. The critical frequency ω_c and the 3-dB bandwidth are defined as function of lattice coefficients k_1 and k_2

$$\omega_c = \arccos(-k_1) \tag{4.4}$$

$$k_2 = \frac{1 - \tan(BW/2)}{1 + \tan(BW/2)}. \tag{4.5}$$

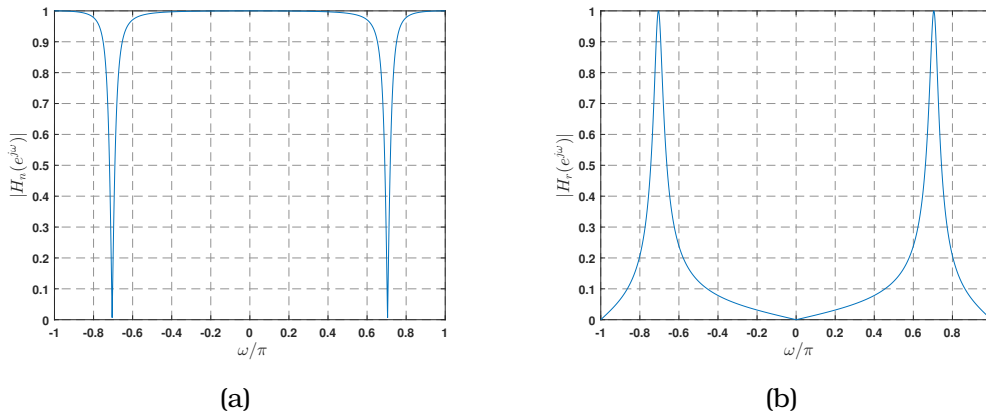


Fig. 4.3 The magnitude response of notch filter ($\|H_n(e^{j\omega})\|$) and perfect resonant filter ($\|H_r(e^{j\omega})\|$).

4.6 Two-Dimensional IIR Notch Filter Design

There are various methods available in the literature for the design and performance analysis of two IIR and FIR notch/multi-notch filters [49, 35, 73, 61, 12, 68, 72, 63]. In this section we present a design procedure for a 2-D IIR notch filter using a 2-D all-pole digital filter. The 2-D all-pole is based on a lattice-ladder structure which is often wont to derive digital filter structures with modular circuitry that is suitable for implementation. Also, from the circuit point of view, we present an implementation of 2-D transfer functions where it is characterized by two lattice coefficients which are expressed in terms of the notch frequency and the 3-dB rejection bandwidth.

The increase of the coefficient k_3 makes the notch filter have a narrower stop bandwidth. The coefficient k_1 can effectively tunes the notch frequency. The advantage of this design is to concept the desired notch filter directly without using any realization approaches which may cost greater computational complexity.

4.6.1 Proposed lattice ladder structure

In this section, we propose a discrete 2-D filter by employing a lattice-type IIR filter [39], which has two delay units z_1^{-1} , z_1^{-1} and an elementary lattice section $z_1 z_2^{-1}$ as shown in figure 4.4. According to figure 4.4 the relationship between input-output is given by

$$\begin{bmatrix} X_3(z_1, z_2) \\ U_3(z_1, z_2) \end{bmatrix} = \begin{bmatrix} 1 & k_3 z_1 z_2^{-1} \\ k_3 & z_1 z_2^{-1} \end{bmatrix} \begin{bmatrix} 1 & k_2 z_1^{-1} \\ k_2 & z_1^{-1} \end{bmatrix} \begin{bmatrix} 1 & k_1 z_1^{-1} \\ k_1 & z_1^{-1} \end{bmatrix} U_0(z_1, z_2) \quad (4.6)$$

$$Y(z_1, z_2) = X_3(z_1, z_2) \vee_3 + X_2(z_1, z_2) \vee_2 + X_1(z_1, z_2) \vee_1 + X_0(z_1, z_2) \vee_0 \quad (4.7)$$

$$U_0(z_1, z_2) = X_0(z_1, z_2) \quad (4.8)$$

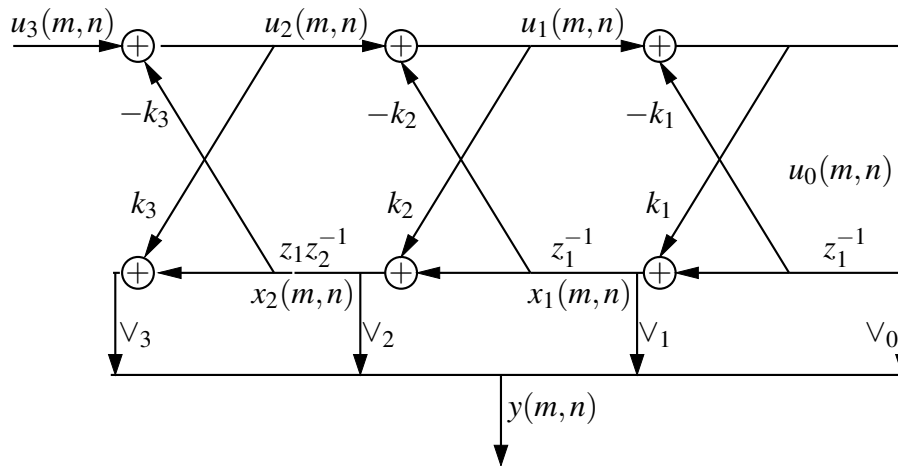


Fig. 4.4 The proposed Lattice-ladder 2-D digital filter.

Using Equations (4.6),(4.7) and (4.8) and figure 4.4, the above transfer function can be computed as follows

$$H_3(z_1, z_2) = \frac{Y(z_1, z_2)}{U_3(z_1, z_2)},$$

$$H_3(z_1, z_2) = \frac{a_1 + (\vee_1 + \vee_2 k_1(1 + k_2) + \vee_3 k_1 k_3(1 + k_2))z_1^{-1} + k_1(1 + k_2)\vee_3 z_2^{-1} + \vee_3 k_2 z_1 z_2^{-1} + (\vee_2 + k_2 k_3 \vee_3)z_1^{-2} + \vee_3 z_1^{-1} z_2^{-1}}{1 + k_1(1 + k_2)z_1^{-1} + k_3 k_1(1 + k_2)z_2^{-1} + k_2 k_3 z_1 z_2^{-1} + k_2 z_1^{-2} + k_3 z_1^{-1} z_2^{-1}}, \quad (4.9)$$

where, $a_1 = \vee_0 + \vee_1 k_1 + \vee_2 k_2 + \vee_3 k_3$.

$k_i, i = 1, \dots, 3$. are reflection coefficients.

$\vee_i, i = 1, \dots, 3$. are ladder network.

If $\vee_i = 0, i = 0, \dots, 2$ and $\vee_3 = 1$, (4.25) can provide filters having all-pass and all-pole characteristics [40]. The 2-D lattice all-pass structure keeps stable if and only if all reflection coefficients satisfy $\|k_i\| < 1$ [39].

From (4.9) and figure 4.5, the transfer function of an all-pole is as follows

$$H_3(z_1, z_2) = \frac{\vee_0}{1 + k_1(1 + k_2)z_1^{-1} + k_3 k_1(1 + k_2)z_2^{-1} + k_2 k_3 z_1 z_2^{-1} + k_2 z_1^{-2} + k_3 z_1^{-1} z_2^{-1}}, \quad (4.10)$$

where the ladder network are $\vee_1 = \vee_2 = \vee_3 = 0$, and $\vee_0 = 1$. The poles of $H_{AP}(e^{j\omega_1}, e^{j\omega_2})$ do not depend on the gain factor \vee_0 and any variations in \vee_0 can not change the response.

4.6.2 Two-Dimensional IIR Notch Filter Design

Generally, The ideal 2-D IIR notch filter $H_{In}(e^{j\omega_1}, e^{j\omega_2})$ obeys the frequency response

$$H_{In}(e^{j\omega_1}, e^{j\omega_2}) \begin{cases} 0, & \text{if } (\omega_1, \omega_2) = (\pm\omega_{1N}, \pm\omega_{2N}) \\ 1, & \text{otherwise} \end{cases} \quad (4.11)$$

where $(\omega_{1N}, \omega_{2N})$ is the notch frequency.

4.6.3 Design Two-Dimensional IIR Notch Filter using an all-pole filter

In this section, 2-D IIR notch filter design using an all pole filter will be investigated. Based on the 2-D all pole filter (4.10), the block diagram of the

2-D IIR notch filter is presented in figure 4.5 and the transfer function can be written as

$$H_{n1}(e^{j\omega_1}, e^{j\omega_2}) = \frac{Y_1(z_1, z_2)}{U_3(z_1, z_2)} = V_0 - H_{AP}(e^{j\omega_1}, e^{j\omega_2}) \quad (4.12)$$

$$H_{n1}(z_1, z_2) = \frac{(k_1(1+k_2)z_1^{-1} + k_3k_1(1+k_2)z_2^{-1} + k_2k_3z_1z_2^{-1} + k_2z_1^{-2} + k_3z_1^{-1}z_2^{-1})V_0}{1 + k_1(1+k_2)z_1^{-1} + k_3k_1(1+k_2)z_2^{-1} + k_2k_3z_1z_2^{-1} + k_2z_1^{-2} + k_3z_1^{-1}z_2^{-1}} \quad (4.13)$$

The transfer function (4.13) may be realized where k_1 , k_2 and k_3 denote the lattice coefficients. The filters to be chosen are IIR notch filter for which there are results about how to avoid distortions. Thus, if BW denote the 3-dB notch band-width obtained [53], ω_0 the center frequency, and $(\omega_{1n}, \omega_{2n})$ the notch frequency, the design equations of the notch filter are

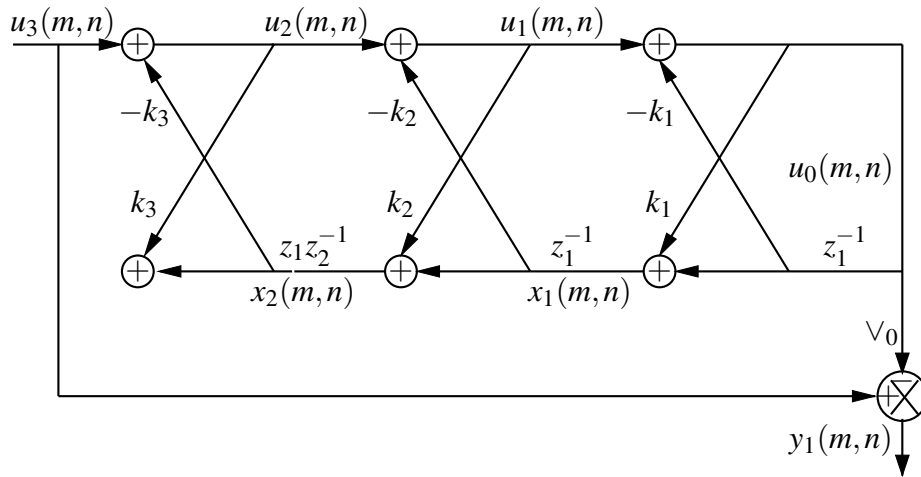


Fig. 4.5 The proposed 2-D IIR Notch Filter structure.

- The coefficient that determines the notch frequency

$$k_1 = -\cos \omega_0, \quad (4.14)$$

- The notch frequency $\omega_{2n} = \omega_0$
- If the frequency ω_0 is positive

$$\omega_{1n} = -\pi + \omega_0. \quad (4.15)$$

If the frequency ω_0 is negative

$$\omega_{1n} = \pi + \omega_0. \quad (4.16)$$

- We take the value of k_2 is more than 0.9997.
- The coefficient that determines the bandwidth of the notch filter

$$k_3 = \frac{1 - \tan(BW/12)}{1 + \tan(BW/12)}. \quad (4.17)$$

In order to keep the magnitude response between one and zero, \forall_0 must be one divided by the maximum value of the magnitude response.

After developing the equations calculating the parameters of the lattice ladder, the design of notch filter is done by knowing 3-dB bandwidth and the center frequency ω_0 .

4.6.4 Parallel of Two-Dimensional IIR Notch Filter

The structure of 2-D notch filter is consisted of two structures of notch filter figure 4.5 in two parallel branches $H_{n1}(z_1, z_2)$ and $H_{n1}(z_2, z_1)$ as in figure 4.6, and the design equations become

- The equations (4.14), (4.15), (4.16) and (4.17) remain the same
- The coefficient that determines the notch frequency $\hat{k}_1 = \cos \omega_0$
- We take the value of \hat{k}_2 is more than 0.9997.
- The coefficient that determines the bandwidth of the notch filter $\hat{k}_3 = k_3$

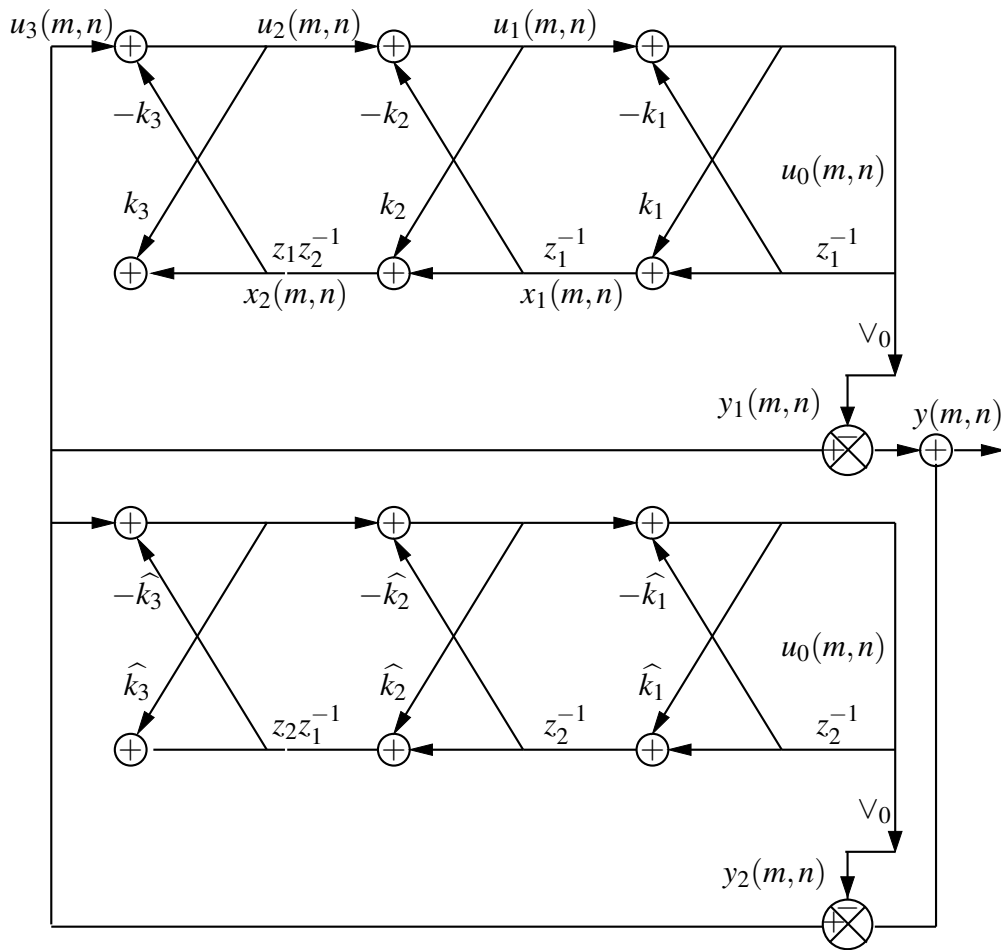


Fig. 4.6 The parallel 2-D IIR Notch Filter structure.

4.6.5 simulation examples

Simulation results are presented as comparisons with the two designs. We choose the $\omega_0 = 0.4\pi$ and a 3-dB notch bandwidth $BW = 0.02\pi$.

- The design of the 2-D IIR notch filter using an all-pole filter

$$k_1 = -\cos(0.4\pi) = -0.3090, (\omega_{1n}, \omega_{2n}) = (-0.6\pi, 0.4\pi),$$

$$k_3 = \frac{1 - \tan(0.02\pi/12)}{1 + \tan(0.02\pi/12)} = 0.9896, \text{ we take } k_2 = 0.99979.$$

Therefore, the 2-D magnitude response $\|H_{n1}(e^{j\omega_1}, e^{j\omega_2})\|$ is presented in figure 4.7. Figure 4.7 shows a 2-D notch filter where the cutoff frequency is localized at $(\omega_{1n}, \omega_{2n}) = (-0.6\pi, 0.4\pi)$

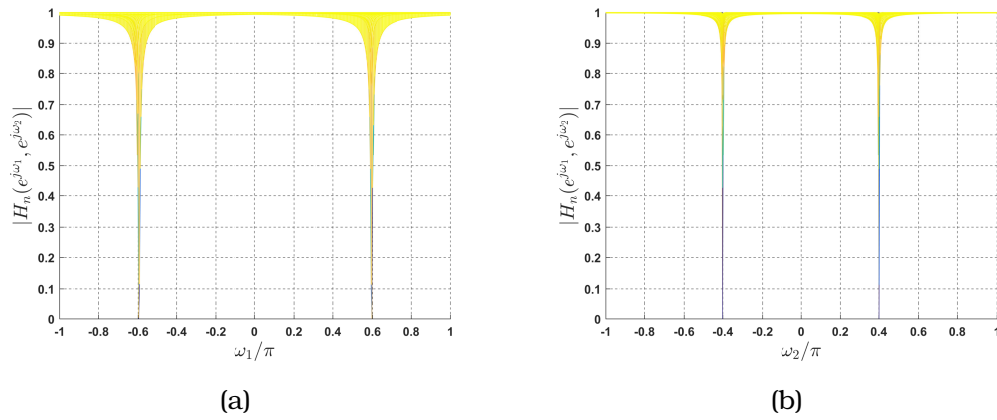


Fig. 4.7 The magnitude response of 2D notch filter $\|H_{n1}(e^{j\omega_1}, e^{j\omega_2})\|$.

We remark that the 3-dB bandwidth vicinity about the notch frequency ω_{1N} and ω_{2N} is not uniform figure 4.7 (a,b).

- The design of the 2-D IIR notch filter using the Parallel Two-Dimensional IIR Notch Filter.

$$k_1 = -\cos(0.4\pi) = -0.3090, \hat{k}_1 = \cos(0.4\pi) = 0.3090,$$

$$\omega_{1n} = -0.6\pi, \hat{k}_3 = k_3 = \frac{1 - \tan(0.02\pi/12)}{1 + \tan(0.02\pi/12)} = 0.9896,$$

we take $\hat{k}_2 = k_2 = 0.99979$.

Therefore, the magnitude response $\|H_N(e^{j\omega_1}, e^{j\omega_2})\|$ is depicted in figure 4.8. Figure 4.8 shows a magnitude response of 2-D notch filter where the cutoff frequency is localized at $(\omega_{1n}, \omega_{2n}) = (-0.6\pi, 0.4\pi)$. We have compared the 3-dB vicinity of ω_1 and ω_2 about the notch frequency for these structures figure 4.5 and figure 4.6 where their magnitudes response are shown in figure 4.7 (a,b) and figure 4.8 (a,b). It has been observed that the realized 3-dB band width succeeds much better in the stopband figure 4.8 (a,b).

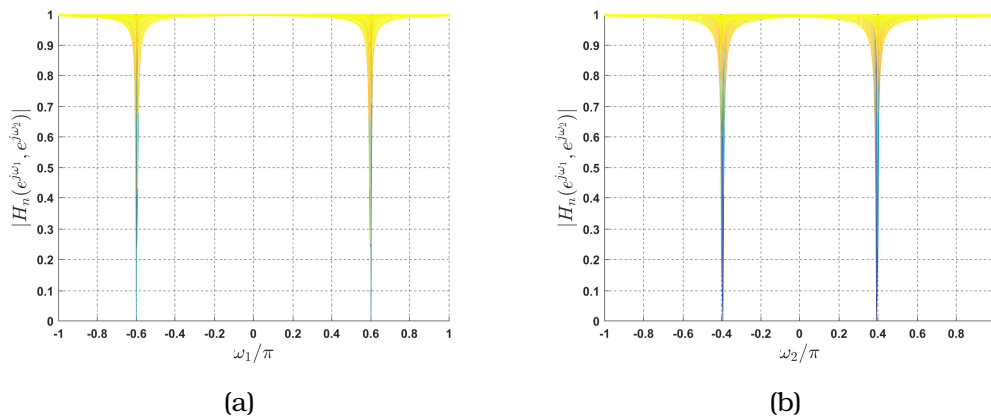
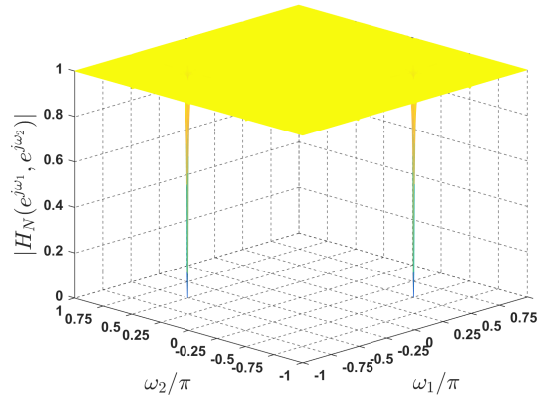


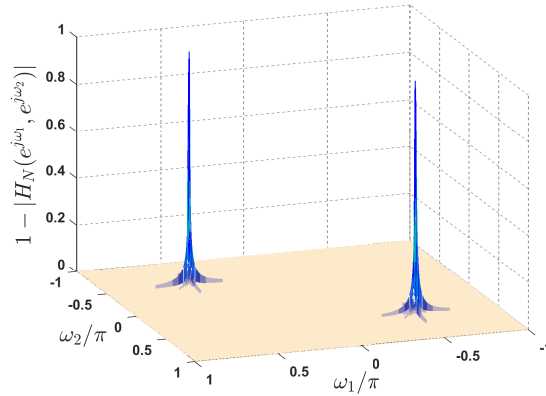
Fig. 4.8 The magnitude response of 2D notch filter $\|H_N(e^{j\omega_1}, e^{j\omega_2})\|$.

4.6.6 2-D IIR notch filter design

The following example is presented to design a 2-D IIR notch filter with the specification as $(\omega_{1N}, \omega_{2N}) = (-0.5\pi, 0.5\pi)$ and $BW = 0.02\pi$. We used the derived equations presented in the subsection (4.6.4) to synthesis the 2-D notch filter magnitude ($\|H_N(e^{j\omega_1}, e^{j\omega_2})\|$). Figure 4.9 (a) show the resultant magnitude response, the resulting design satisfies the specification where, the magnitude response ($\|H_N(e^{j\omega_1}, e^{j\omega_2})\|$) has flat response over the usable range (ω_1, ω_2) with the exception of notch frequency $(\omega_{1N}, \omega_{2N}) = (-0.5\pi, 0.5\pi)$. To achieve a better efficiency of the proposed notch filter, we should illustrate the loss $(1 - \|H_N(e^{j\omega_1}, e^{j\omega_2})\|)$, the loss is presented in figure 4.9 (b), the frequency response has no ripple in the pass region even in the area of the notch frequencies, which is more noticeable in figure 4.9 (b).



(a)



(b)

Fig. 4.9 (a) The magnitude response of 2-D notch filter $\|H_N(e^{j\omega_1}, e^{j\omega_2})\|$, (b) The loss $(1 - \|H_N(e^{j\omega_1}, e^{j\omega_2})\|)$ of the designed notch filter ,with $(\omega_{1N}, \omega_{2N}) = (-0.5\pi, 0.5\pi)$.

4.6.7 Removing interference of an image

Consider the test image I in figure 4.10 (a), I is the “Lena” (512 by 512) black and white. The degraded image I_n in figure 4.10 (b) is generated by (4.18).

$$I_n = I + 80 \cos(-0.5\pi n + 0.5\pi m) \tag{4.18}$$

Due to the sinusoidal interference, we see a clear pair of symmetric peak impulses in the Fourier spectrum of the degraded image I_n positioned at $(-0.5\pi, 0.5\pi)$ and $(0.5\pi, -0.5\pi)$ in figure 4.10 (c). We processed the corrupted

image by the proposed 2-D notch filter ($\|H_N(e^{j\omega_1}, e^{j\omega_2})\|$), the output image is seen clearly, which is shown in figure 4.10 (d), and we can observe that the interference has been removed.

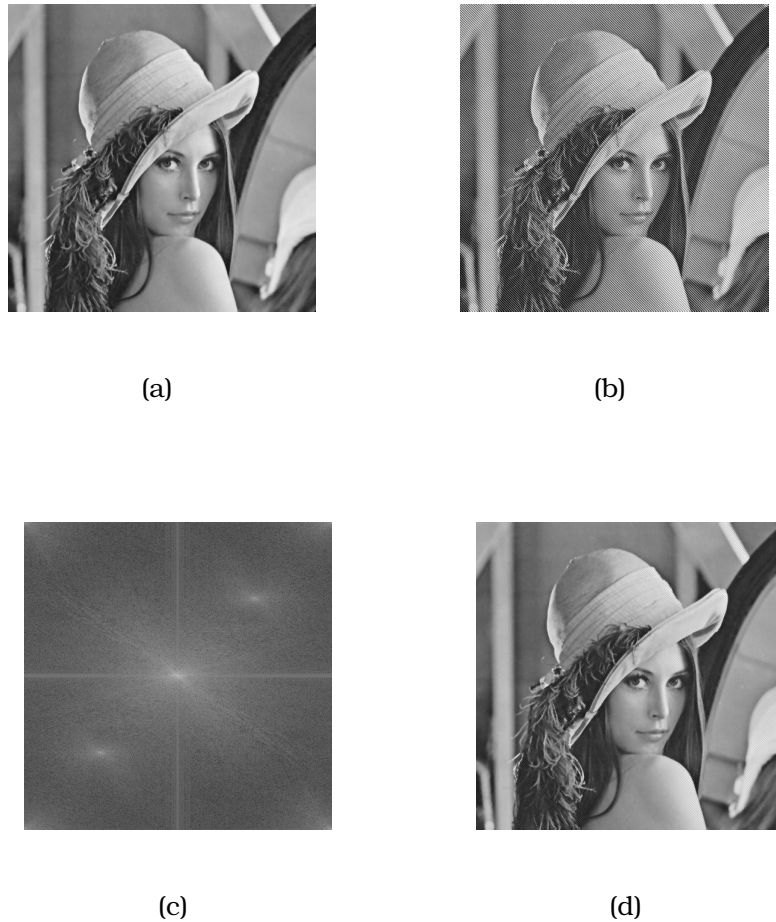


Fig. 4.10 Example of single sinusoidal interference removal. (a) Original image (b) Corrupted image (c) Image with interference DFT magnitude (d) Image restored by using 2-D IIR notch filter $\|H_N(e^{j\omega_1}, e^{j\omega_2})\|$.

4.6.8 Interpretation

This section has suggested a new design procedure of 2-D IIR notch filters with relatively low ladder-lattice structural complexity. The digital notch filter is implemented as two all-pole parallel system. The frequency response has a uniformly flat passband gain and zero gains at the notch frequencies. Besides, there are no ripples appears in the passband. Finally, the design of

the proposed 2-D notch filter is presented, and an application example to remove the contamination on an image.

4.7 3-D IIR Notch Filter Design

Digital notch filters are designed to reject a particular frequency highly while leaving other frequency unaffected [13, 38, 48, 50, 64, 31, 51]. This section addresses the design problem of a 3-D IIR notch filter [8, 7]. The proposed filter is realized using two filters. The first one is an IIR filter based on all-pass filter which can be designed and implemented via lattice structure. It allows us to adjust the 3-dB rejection bandwidth of the notch filter with the lattice coefficient independently of the second filter design. The second one is a 3-D spatial straight line filter [9] and it is designed to localize the notch frequency. In addition, a 3-D analogue Prototype filter is designed using frequency transformation.

4.7.1 3-D IIR All-pass Filter Design

Figure 4.11 shows the proposed lattice structure for constructing a 3-D IIR all-pass digital filter with order $1 \times 1 \times 1$. This structure has three basic lattice sections z_1^{-1} , z_2^{-1} and $z_1 z_3^{-1}$. The input-output relationship of the proposed lattice structure shown in figure 4.11 is given by the following matrix representation

$$\begin{bmatrix} X_3(z_1, z_2, z_3) \\ U_3(z_1, z_2, z_3) \end{bmatrix} = \begin{bmatrix} 1 & k_2 z_1 z_3^{-1} \\ k_2 & z_1 z_3^{-1} \end{bmatrix} \begin{bmatrix} 1 & k_1 z_2^{-1} \\ k_1 & z_2^{-1} \end{bmatrix} \begin{bmatrix} 1 & k_0 z_1^{-1} \\ k_0 & z_1^{-1} \end{bmatrix} Y(z_1, z_2, z_3) \quad (4.19)$$

From (4.19), one can get the expressions

$$X_3(z_1, z_2, z_3) = T(z_1, z_2, z_3) Y(z_1, z_2, z_3) \quad (4.20)$$

$$U_3(z_1, z_2, z_3) = S(z_1, z_2, z_3) Y(z_1, z_2, z_3) \quad (4.21)$$

where

$$T(z_1, z_2, z_3) = 1 + k_0 k_1 z_2^{-1} + k_0 z_1^{-1} + k_1 z_1^{-1} z_2^{-1} + k_1 k_2 z_1 z_3^{-1} + k_0 k_2 z_1 z_2^{-1} z_3^{-1} + k_2 z_2^{-1} z_3^{-1} + k_0 k_1 k_2 z_3^{-1}$$

$$S(z_1, z_2, z_3) = k_2 + k_2 k_0 k_1 z_1 z_2^{-1} + k_1 z_2 z_3^{-1} + k_0 z_1 z_3^{-1} + k_2 k_0 z_1^{-1} + k_2 k_1 z_2^{-1} + k_0 z_2 z_3^{-1} z_1^{-1} + z_3^{-1}$$

After rearrangement, one can get the following relationship

$$S(z_1, z_2, z_3) = z_2^{-1} z_3^{-1} T(z_1^{-1}, z_2^{-1}, z_3^{-1}) \quad (4.22)$$

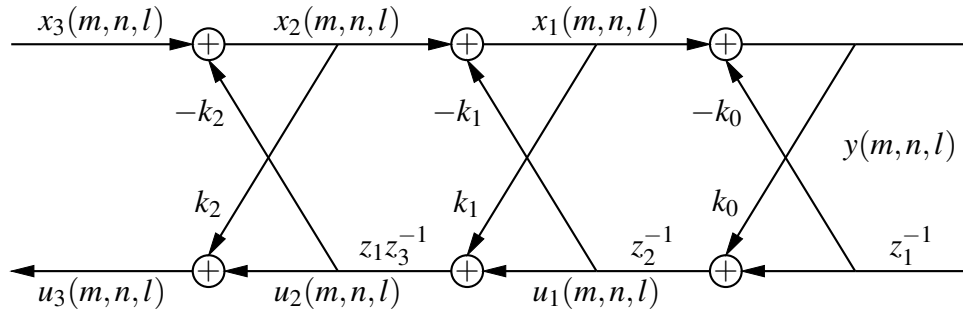


Fig. 4.11 Proposed 3-D recursive digital all-pass filter with order $1 \times 1 \times 1$.

From (4.20) and (4.21), one can construct the forward transfer function of 3-D recursive digital all-pass filter of order $1 \times 1 \times 1$ as follows

$$H_A(z_1, z_2, z_3) = \frac{U_3(z_1, z_2, z_3)}{X_3(z_1, z_2, z_3)} = z_2^{-1} z_3^{-1} \frac{T(z_1, z_2, z_3)}{T(z_1^{-1}, z_2^{-1}, z_3^{-1})} \quad (4.23)$$

It should be noted that the numerator and denominator polynomials of $H_A(z_1, z_2, z_3)$ are mirror images of each other, which is a general property of all-pass system.

4.7.2 3-D IIR filter design

Based on the transfer function of the all-pass filter given by 4.23, we have proposed an IIR filter shown in figure 4.12 and given by the following transfer function

$$H_p(z_1, z_2, z_3) = \frac{1}{2} (1 - H_A(z_1, z_2, z_3)) \quad (4.24)$$

This filter is the key of our design and has the advantages of an all-pass filter with computationally coefficient lattice filter realization and very low sensitivity.

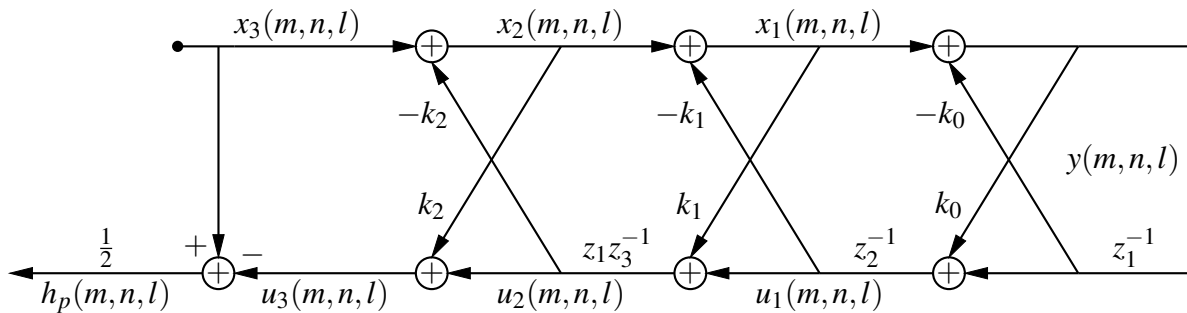


Fig. 4.12 Implementation of $H_p(z_1, z_2, z_3)$.

Besides, the rejection bandwidth can be adjusted by the lattice coefficient k_2 where the coefficients k_0 and k_1 are kept as small as possible. Figure 4.13 illustrates the 2-D magnitude response of $H_p(z_1, z_2, z_3)$ for different values of k_2 where ω_3 is chosen to be fixed. It can be remarked that the rejection bandwidth progressively decreases as k_2 increases. The next subsection presents the straight line filter.

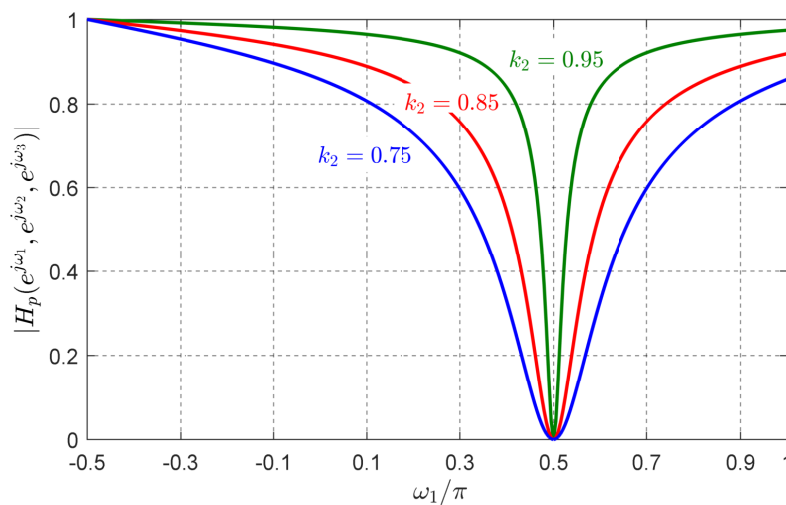


Fig. 4.13 The rejection bandwidth can be adjusted by varying the coefficient k_2 .

4.7.3 3-D IIR spatial straight line filter design

Figure 4.14 illustrates a first-order continuous-domain 3-D inductance-resistance system [9]. The voltage transfer function of this system is given

by

$$T_1(s_1, s_2, s_3) = \frac{U(s_1, s_2, s_3)}{V(s_1, s_2, s_3)} = \frac{R}{R + s_1L_1 + s_2L_2 + s_3L_3} \quad (4.25)$$

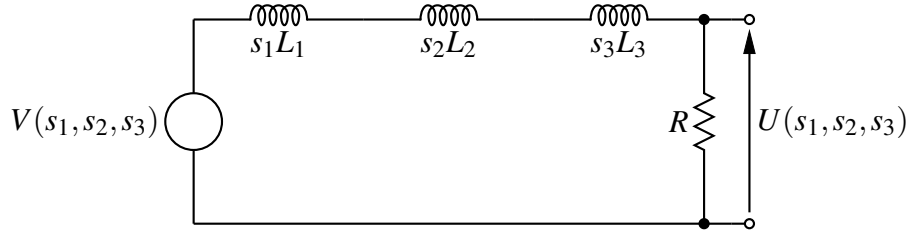


Fig. 4.14 First order 3-D inductance resistance system.

The frequency response of (4.25) is given by

$$T_1(j\omega_1, j\omega_2, j\omega_3) = \frac{R}{R + j(\omega_1L_1 + \omega_2L_2 + \omega_3L_3)} \quad (4.26)$$

The magnitude response of $T_1(j\omega_1, j\omega_2, j\omega_3)$ has a maximum value of unity where

$$\omega_1L_1 + \omega_2L_2 + \omega_3L_3 = 0 \quad (\text{Resonant plane}) \quad (4.27)$$

and $T_1(j\omega_1, j\omega_2, j\omega_3) = \frac{1}{\sqrt{2}}$

$$\omega_1L_1 + \omega_2L_2 + \omega_3L_3 = \pm R \quad (-3\text{dB planes}) \quad (4.28)$$

Discrete version of the planar-resonant filters are obtained by subjecting the analogue 3-D transfer function $T_1(s_1, s_2, s_3)$ to the triple bilinear transformation

$$s_i = \frac{z_i - 1}{z_i + 1}, \quad i = 1, 2, 3 \quad (4.29)$$

The resulting discrete transfer function

$$H_s(z_1, z_2, z_3) = \|T_1(s_1, s_2, s_3)\|_{s_i = \frac{z_i - 1}{z_i + 1}} \quad (4.30)$$

where we replace s_i by $\frac{(z_i - 1)}{(z_i + 1)}$, giving for the discrete planar resonant filters, after multiplying the numerator and denominator of the above transfer function by $(z_1 + 1)(z_2 + 1)(z_3 + 1)$, one can get

$$H_s(z_1, z_2, z_3) = \frac{R(z_1 + 1)(z_2 + 1)(z_3 + 1)}{D_s(z_1, z_2, z_3)} \quad (4.31)$$

where $D_s(z_1, z_2, z_3) = (R(z_1 + 1) + L_1(z_1 - 1))(z_2 + 1)(z_3 + 1) + (L_2(z_2 - 1)(z_3 + 1) + L_3(z_2 + 1)(z_3 - 1))(z_1 + 1)$.

4.7.4 Implementation and design 3-D IIR Notch filter

3-D IIR Notch Filter Design

In this section, a new method for the design of notch filter is presented. The ideal 3-D IIR notch filter is characterized by a unit gain at all frequencies except at the sinusoidal frequencies in which their gain is zero

$$H_d(e^{j\omega_1}, e^{j\omega_2}, e^{j\omega_3}) = \begin{cases} 0, & \text{if } (\omega_1, \omega_2, \omega_3) = (\omega_{1N}, \omega_{2N}, \omega_{3N}) \\ 1, & \text{otherwise} \end{cases} \quad (4.32)$$

where $(\omega_{1N}, \omega_{2N}, \omega_{3N})$ is the notch frequency.

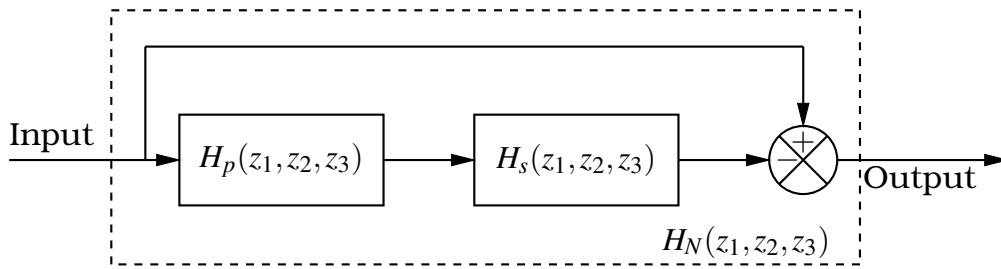


Fig. 4.15 The 3-D IIR notch filter design.

Figure 4.15 shows the proposed scheme of 3-D IIR notch filter, which includes two filters: one is 3-D spatial straight line filter $H_s(z_1, z_2, z_3)$ and the other is based on all-pass filter $H_p(z_1, z_2, z_3)$. From the block diagram shown in figure 4.15, [63] the transfer function of the 3-D IIR notch filter is given by

$$H_N(z_1, z_2, z_3) = 1 - H_p(z_1, z_2, z_3)H_s(z_1, z_2, z_2) \quad (4.33)$$

For a given notch frequency $(\omega_{1N}, \omega_{2N})$, one can distinguish two cases as follows:

- If the frequency (ω_{1N}) is positive:

$$\omega_{3N} = \pi - \omega_{1N} \quad (4.34)$$

- If the frequency (ω_{1N}) is negative:

$$\omega_{3N} = -(\pi + \omega_{1N}) \quad (4.35)$$

Hence, if we properly choose the parameters as

$$L_1 = -\tan\left(\frac{\omega_{1N}}{2}\right) \quad (4.36)$$

$$L_2 = \tan\left(\frac{\omega_{2N}}{2}\right) \quad (4.37)$$

and L_3 is as small as possible, then $H_s(z_1, z_2, z_3)$ will be a spatial straight line filter whose resonant line pass through the notch frequency point ($\omega_{1N}, \omega_{2N}, \omega_{3N}$) exactly although there exists bending effect due to the triple bilinear transformation [63]. This parameter choice and the equations (4.34) and (4.35) are the key step of this design procedure. In order to achieve bounded-input bounded-output (BIBO) stability of the system [9], the parameters L_1 , L_2 and L_3 have to be nonnegative. The design and implementation of 3-D IIR notch filter can be summarized as follows:

1. Specify the notch frequency (ω_{1N}, ω_{2N}) and compute ω_{3N} .
2. choose the coefficients k_0 , k_1 as small as possible and k_2 between 0.85 and 0.95 to have a very narrow 3-dB rejection bandwidth of the notch filter.
3. choose the parameter of the spatial straight line filter L_1 , L_2 and L_3 as small as possible. The appropriate value of R is less or equal to 0.01.
4. Construct the transfer function from equations (4.24) and (4.30).
5. The transfer function of the 3-D IIR notch filter can be obtained using (4.33).

Numerical Example

Once the transfer function of the 3-D IIR notch filter has been designed, the magnitude response is consequently obtained. Since it is difficult to illustrate all 3-D magnitude responses in one figure, the 2-D magnitude response will be presented instead by fixing one dimension. In this case, ω_{3N} is chosen to be fixed. As a result, the magnitude response of $H_N(z_1, z_2, z_3)$

can be presented, we show the 2-D slice for various frequencies ω_3 . The magnitude gain is obviously unity for all ω_3 , except $\omega_3 = \omega_{3N}$. At $\omega_3 = \omega_{3N}$, the notch frequency operates at $(\omega_1, \omega_2) = (\omega_{1N}, \omega_{2N})$. In this example, the design steps described above are used to define the 3-D IIR notch filter for the notch frequency $(\omega_{1N}, \omega_{2N}) = (-0.6\pi, 0.5\pi)$, $\omega_{3N} = -0.4\pi$.

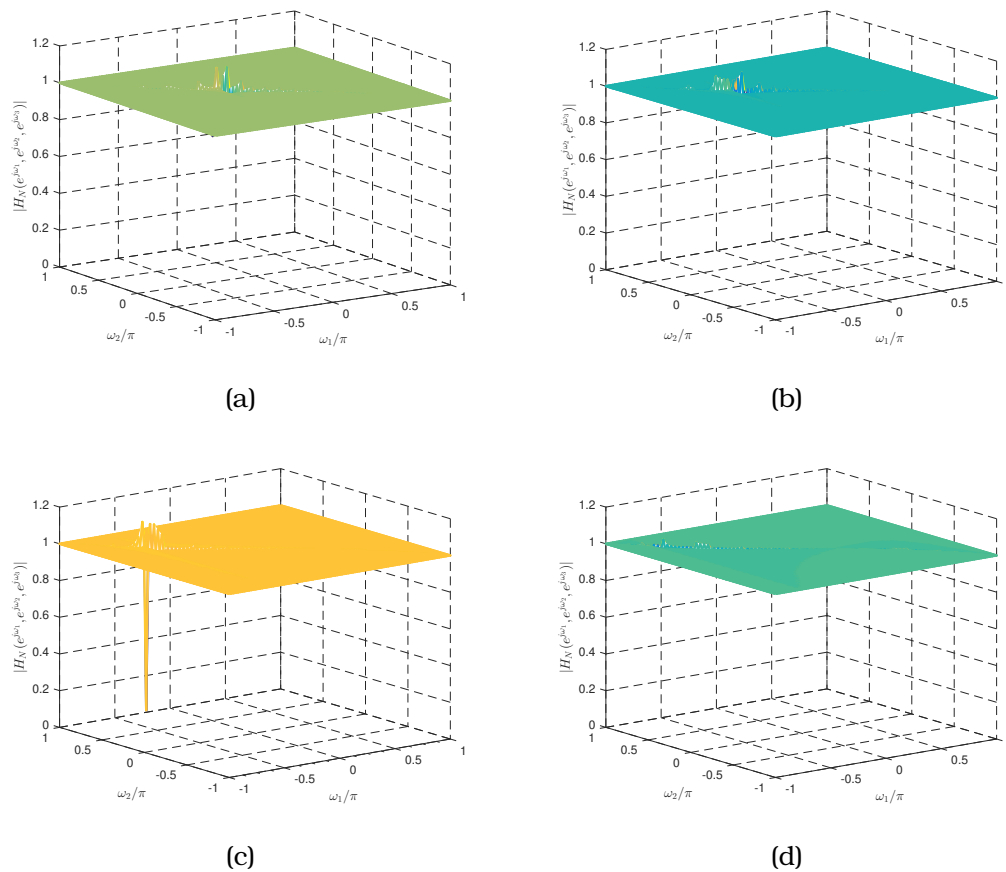


Fig. 4.16 Three-dimensional magnitude response with the notch frequency is $(-0.6\pi, 0.5\pi, -0.4\pi)$. (a) $\omega_3 = -0.8\pi$. (b) $\omega_3 = -0.6\pi$. (c) $\omega_3 = -0.4\pi$. (d) $\omega_3 = -0.2\pi$.

The filter parameters are chosen as $k_0 = 0.001$, $k_1 = 0.005$, $k_2 = 0.95$, $R = 0.03$, $L_3 = 0.0005$. Figure 4.16 shows the magnitude of the notch filter. One can remark that $\|H_N(e^{j\omega_1}, e^{j\omega_2}, e^{-j0.4\pi})\|$ has a unit gain at all frequencies (ω_1, ω_2) figure 4.16 (a),(b) and (d), except at $(-0.6\pi, 0.5\pi)$ where gain is zero, figure 4.16 (c). The notch filter operates at $(\omega_{1N}, \omega_{2N}, \omega_{3N}) = (-0.6\pi, 0.5\pi, -0.4\pi)$.

Interpretation

In this section, a new design procedure of 3-D IIR notch filter has been presented based on a circuit of 3-D IIR all-pass filter with order $1 \times 1 \times 1$. We have developed a new algebraic method for this design. The proposed solution is in closed-form, and it does not require any iterative procedure or optimization techniques. It has been shown, by an example the notch filters can be easily designed.

Chapter 5

Conclusions

In the introductory chapter 1, the definition of some N-D signals and systems with a variety of operations which will serve as building blocks for the development of more complicated signals and systems. Other definitions of the stability, the Roesser's state space and the realization of digital filters is presented. In chapter 2, review of the minimal state-space realization problem. There are pressing needs to reduce the hardware requirements as much as possible because, various problems such as round-off error analysis, coefficient sensitivity, optimization, ...etc., can be studied much more effectively using the state space approach. The aim of the minimal state-space realization problem is to find a state-space model of minimal size of the given system.

In chapter 3, we propose two structures in lattice and ladder-lattice form and find the minimal state-space realization of those structures. The lattice filter is classified as an important structure in digital signal processing. In fact, it minimizes the computation complexity, reduces the finite word length, and requires less hardware compared to the direct form digital filter with similar design specifications.

In chapter 4, the structures of the latter chapter is considered to realize notch filters type. First, characteristics and applications of notch filter are presented. Then, the 2-D IIR digital notch filter is implemented, a 2-D transfer functions is characterized by two lattice coefficients which are expressed in terms of the notch frequency and the 3-dB rejection bandwidth. The increase of the coefficient k_3 makes the notch filter have a narrower stop bandwidth. The coefficient k_1 can effectively tunes the notch frequency. The frequency response has an uniformly flat passband gain and zero gains

at the notch frequencies. Besides, there are no ripples appears in the passband. An application example to remove the contamination on an image is presented which improve the effectiveness of the proposed procedure. In the last section of chapter 4 a new design procedure of 3-D IIR notch filter has been presented based on two filters design i) An 3-D IIR filter based on circuit of 3-D IIR all-pass filter with order $1 \times 1 \times 1$, and ii) A straight line filter designed by frequency transformation of 3-D analogue prototype filter. The proposed solution is in closed-form, and it does not require any iterative procedure or optimization techniques.

References

- [1] Ahmadi, M. and Antoniou, A. (1980). Design of n-dimensional digital filters with variable cutoff boundary. In *Proc. IEEE Int. Symp. Circuits Syst.*, pages 217–220.
- [2] Antoniou, G., Paraskevopoulos, P., and Varoufakis, S. (1988). Minimal state-space realization of factorable 2-d transfer functions. *IEEE transactions on circuits and systems*, 35(8):1055–1058.
- [3] Antoniou, G., Varoufakis, S., and Paraskevopoulos, P. (1986). State-space realization of 2-d systems via continued fraction expansion. *IEEE transactions on circuits and systems*, 33(9):926–930.
- [4] Antoniou, G. E. (2001). Generalized one-multiplier lattice discrete 2-d filters: Minimal circuit and state-space realization. *IEEE Transactions on Circuits and Systems I: Fundamental Theory and Applications*, 48(2):215–218.
- [5] Antoniou, G. E. (2004). On the realization of 2d lattice-ladder discrete filters. *Journal of Circuits, Systems, and Computers*, 13(05):1079–1083.
- [6] B. De Moor, P. Van Overschee, W. F. (1999). Algorithms for subspace state-space system identification: an overview. in: *B. Datta (Ed.), Applied and Computational Control, Signals, and Circuits, Vol. 1, Birkhauser, Boston, 1999, pp. 271-335 (Chapter 6)*.
- [7] Bose, N. (2007). Feature-multidimensional systems and signal processing: Good theory for good practice. *IEEE Circuits and Systems Magazine*, 7(4):20–41.
- [8] Bose, N. K. (1982). *Applied multidimensional systems theory*. Springer.
- [9] Bruton, L. and Bartley, N. (1985). Three-dimensional image processing using the concept of network resonance. *IEEE Transactions on Circuits and Systems*, 32(7):664–672.
- [10] Bultheel, A. and Moor, B. (2000). Rational approximation in linear systems and control. *Journal of Computational and Applied Mathematics*, 121(1):355 – 378.
- [11] Chen, C. (1984). *Linear system theory and design* (new york: Holt, reinhart and winston). e.

- [12] Chinoun, A., Mitiche, L., and Adamou-Mitiche, A. B. H. (2019). New design approach of three-dimensional iir notch filter using all-pass sections. *Australian Journal of Electrical and Electronics Engineering*, 16(4):276–280.
- [13] Cousseau, J. E., Werner, S., and Donate, P. D. (2007). Factorized all-pass based iir adaptive notch filters. *IEEE Transactions on Signal Processing*, 55(11):5225–5236.
- [14] D’Alotto, L. A., Giardina, C. R., and Luo, H. (1998). *A unified signal algebra approach to two-dimensional parallel digital signal processing*, volume 210. CRC Press.
- [15] Dattorro, J. (1997). Effect design, part 1: Reverberator and other filters. *Journal of the Audio Engineering Society*, 45(9):660–684.
- [16] De Schutter, B. (2000). Minimal state-space realization in linear system theory: an overview. *Journal of computational and applied mathematics*, 121(1-2):331–354.
- [17] Dewilde, P. and Van der Veen, A.-J. (1998). *Time-varying systems and computations*. Springer Science & Business Media.
- [18] Drynkin, V. N. (1995). Real-time design of n-dimensional digital filters for image processing. In *Digital Photogrammetry and Remote Sensing’95*, volume 2646, pages 240–249. International Society for Optics and Photonics.
- [19] Dudgeon, D. E. and Mersereau, R. M. (1984). *Multidimensional digital signal processing*.
- [20] Edussooriya, C. U., Dansereau, D. G., Bruton, L. T., and Agathoklis, P. (2015). Five-dimensional depth-velocity filtering for enhancing moving objects in light field videos. *IEEE Transactions on Signal Processing*, 63(8):2151–2163.
- [21] Galkowski, K. (1981). The state-space realization of an n-dimensional transfer function. *International Journal of Circuit Theory and Applications*, 9(2):189–197.
- [22] Galkowski, K. (2001). *State-space realisations of linear 2-D systems with extensions to the general nD (n > 2) case*, volume 263. Springer Science & Business Media.
- [23] Gantmakher, F. (1959). *The Theory of Matrices: 374p. v. 2., 276p.* The Theory of Matrices. Chelsea Publishing Company.
- [24] Gilbert, E. G. (1963). Controllability and observability in multivariable control systems. *Journal of the Society for Industrial and Applied Mathematics Series A Control*, 1(2):128–151.

- [25] Givone, D. D. and Roesser, R. P. (1973). Minimization of multidimensional linear iterative circuits. *IEEE Transactions on Computers*, 100(7):673–678.
- [26] GLOVER, K. (1984). All optimal hankel-norm approximations of linear multivariable systems and their l_1 -error bounds†. *International Journal of Control*, 39(6):1115–1193.
- [27] Gohberg, I. and Kaashoek, M. (1986). On minimality and stable minimality of time-varying linear systems with well-posed boundary conditions. *International Journal of Control*, 43(5):1401–1411.
- [28] Gray, A. and Markel, J. (1973). Digital lattice and ladder filter synthesis. *IEEE Transactions on audio and electroacoustics*, 21(6):491–500.
- [29] HO, . L., . K. R. E. (1966). Editorial: Effective construction of linear state-variable models from input/output functions. *at - Automatisierungstechnik*, 14(1-12), 545-548.
- [30] Isidori, A. (2013). *Nonlinear control systems*. Springer Science & Business Media.
- [31] Jaiswal, V. K. (2018). A novel notch filter using wavelet tranform and statistical curve fitting. In *2018 IEEMA Engineer Infinite Conference (eTech-NxT)*, pages 1–6. IEEE.
- [32] Joshi, Y. and Roy, S. D. (1997). Design of iir digital notch filters. *Circuits, Systems and Signal Processing*, 16(4):415–427.
- [33] Kaczorek, T. (1999). Two-dimensional linear systems. In *Advances in Control*, pages 283–284. Springer.
- [34] Kalman, R. E. (1963). Mathematical description of linear dynamical systems. *Journal of the Society for Industrial and Applied Mathematics Series A Control*, 1(2):152–192.
- [35] Kocoń, S. and Piskorowski, J. (2014). Time-varying iir multi-notch filter based on all-pass filter prototype. pages 112–118.
- [36] Kousoulis, M. and Antoniou, G. (2016). Realization of 4d lattice-ladder digital filters. In *2016 IEEE 7th Latin American Symposium on Circuits & Systems (LASCAS)*, pages 15–18. IEEE.
- [37] Kousoulis, M., Coutras, C. A., and Antoniou, G. (2019). 4d bidirectional lattice digital filters. In *2019 IEEE 10th Latin American Symposium on Circuits & Systems (LASCAS)*, pages 205–208. IEEE.
- [38] Kwan, H. K. and Lui, Y. C. (1989). Lattice implementation of two-dimensional recursive digital filters. *IEEE Transactions on Circuits and Systems*, 36(3):383–386.

- [39] Lee, J. and Du, J. (2017). Lattice structure realization for the design of 2-d digital allpass filters with general causality. *IEEE Transactions on Circuits and Systems I: Regular Papers*, 64(2):419–431.
- [40] Lee, J.-H. and Yang, Y.-H. (2011). General lattice structures of 2-d recursive digital filters. In *2011 IEEE 54th International Midwest Symposium on Circuits and Systems (MWSCAS)*, pages 1–4. IEEE.
- [41] Lennart Souchon (Decembre 1975). *STRUCTURES, ANALYSIS AND DESIGN OF N-DIMENSIONAL RECURSIVE DIGITAL FILTERS*.
- [42] Lim, J. S. (1990). Two-dimensional signal and image processing. *Englewood Cliffs, NJ, Prentice Hall, 1990, 710 p.*
- [43] L.Ljung (1999). *System Identification: Theory for the User, 2nd Edition Prentice-Hall, Upper Saddle River, NJ, 1999.*
- [44] Lu, W.-S. and Lee, E. (1983). Stability analysis for two-dimensional systems. *IEEE Transactions on circuits and systems*, 30(7):455–461.
- [45] MANIKOPOULOS, C. N., MENTZELOPOULOU, S. E., and ANTONIOU, E. (1991). Minimal circuit and state space realization of three-term separable denominator 2-d filters. *International Journal of Electronics*, 71(5):723–731.
- [46] Mayne, D. (1973). An elementary derivation of rosenbrock’s minimal realization algorithm. *IEEE Transactions on Automatic Control*, 18(3):306–307.
- [47] Mitiche, L. and Adamou-Mitiche, A. B. H. (2014). An efficient low order model for two-dimensional digital systems: Application to the 2d digital filters. *Journal of King Saud University-Computer and Information Sciences*, 26(3):308–318.
- [48] Pei, S., Guo, B., and Lu, W. (2016). Narrowband notch filter using feedback structure tips tricks. *IEEE Signal Processing Magazine*, 33(3):115–118.
- [49] Pei, S., Lu, W., and Guo, B. (2017a). Pole-zero assignment of all-pass-based notch filters. *IEEE Transactions on Circuits and Systems II: Express Briefs*, 64(4):477–481.
- [50] Pei, S., Lu, W., and Guo, B. (2017b). Pole-zero assignment of all-pass-based notch filters. *IEEE Transactions on Circuits and Systems II: Express Briefs*, 64(4):477–481.
- [51] Piyachaiyakul, N. and Charoenlarnnoppa, C. (2013). Design of three-dimensional adaptive iir notch filters. *Multidimensional Systems and Signal Processing*, 24(3):435–446.
- [52] Raita-Aho, T., Saramaki, T., and Vainio, O. (1994). A digital filter chip for ecg signal processing. *IEEE Transactions on instrumentation and measurement*, 43(4):644–649.

- [53] Regalia, P. and Mitra, S. (1987). Tunable digital frequency response equalization filters. *IEEE Transactions on Acoustics, Speech, and Signal Processing*, 35(1):118–120.
- [54] Regalia, P. A., Mitra, S. K., and Vaidyanathan, P. (1988). The digital all-pass filter: A versatile signal processing building block. *Proceedings of the IEEE*, 76(1):19–37.
- [55] Rissanen, J. (1971). Recursive identification of linear systems. *SIAM Journal on Control*, 9(3):420–430.
- [56] Roesser, R. (1975). A discrete state-space model for linear image processing. *IEEE Transactions on Automatic Control*, 20(1):1–10.
- [57] Rosenbrock, H. (1970). *State-space and Multivariable Theory*. Studies in dynamical systems. Wiley Interscience Division.
- [58] Schutter, G. J. O. D. (1999). *The minimal realization problem in the max-plus algebra*. Open Problems in Mathematical Systems and Control Theory, Springer, London, 1999, pp. 157-162 (Chapter 32).
- [59] Silverman, L. (1966). Structural properties of time-variable linear systems.
- [60] Silverman, L. (1971). Realization of linear dynamical systems. *IEEE Transactions on Automatic Control*, 16(6):554–567.
- [61] Soo-Chang Pei, Wu-Sheng Lu, and Chien-Cheng Tseng (1997). Analytical two-dimensional iir notch filter design using outer product expansion. *IEEE Transactions on Circuits and Systems II: Analog and Digital Signal Processing*, 44(9):765–768.
- [62] S.PACE, I. and BARNETT, S. (1974). Part ii minimal realization. *International Journal of Systems Science*, 5(5):413–424.
- [63] S.PeI and Tseng, C. . (1993). Two dimensional iir and fir digital notch filter design. pages 890–893 vol.1.
- [64] Stančić, G. and Nikolić, S. (2013). Design of digital recursive notch filter with linear phase characteristic. In *2013 11th International Conference on Telecommunications in Modern Satellite, Cable and Broadcasting Services (TELSIKS)*, volume 1, pages 69–72. IEEE.
- [65] Sussmann, H. J. (1976). Existence and uniqueness of minimal realizations of nonlinear systems. *Mathematical Systems Theory*, 10(1):263–284.
- [66] Tether, A. (1970). Construction of minimal linear state-variable models from finite input-output data. *IEEE Transactions on Automatic Control*, 15(4):427–436.
- [67] Tether, A. (1970). Construction of minimal linear state-variable models from finite input-output data. *IEEE Transactions on Automatic Control*, 15(4):427–436.

- [68] Tseng, C. and Lee, S. (2019). Closed-form design of digital fir notch filter using chebyshev polynomial. pages 287–288.
- [69] Varoufakis, S., Paraskevopoulos, P., and Antoniou, G. (1987). On the minimal state-space realizations of all-pole and all-zero 2-d systems. *IEEE transactions on circuits and systems*, 34(3):289–292.
- [70] Vlcek, M. and Zahradnik, P. (2001). Digital multiple notch filters performance. In *Proceedings of the 15th European Conference on Circuit Theory and Design ECCTD'01*, pages 49–52.
- [71] Woods, J. W. (2006). *Multidimensional signal, image, and video processing and coding*. Elsevier.
- [72] Wysocka-Schillak, F. (2007). Design of equiripple 2-d linear-phase fir notch filters. pages 112–115.
- [73] Yan, S., Sun, L., and Xu, L. (2015). 2-d zero-phase iir notch filters design based on state-space representation of 2-d frequency transformation. pages 2369–2370.
- [74] Youla, D. C. (1966). N-port synthesis via reactance extraction-part i. *IEEE International Conuention Record*, 7:183–205.
- [75] Zahradník, P. and Vlcek, M. (2006). An analytical procedure for critical frequency tuning of fir filters. *IEEE Transactions on Circuits and Systems II: Express Briefs*, 53(1):72–76.
- [76] . L. Ho, R. K. (1965). Editorial: Effective construction of linear state-variable models from input/output functions.

Appendix A

Proof of conditions for BIBO stability

Prove that,

$$S = \sum_{(-\infty \leq \bar{n} \leq \infty)} \sum \dots \sum |h(\bar{n})| < \infty. \quad (\text{A.1})$$

is a necessary and sufficient condition for BIBO stability. If (A.1) is true and if for a bounded input $x(\bar{n})$, i.e., $|x(\bar{n})| < M$ for all (\bar{n}) , then

$$|y(\bar{n})| = \left| \sum_{(-\infty \leq \bar{m} \leq \infty)} \sum \dots \sum h(\bar{m})x(\bar{n} - \bar{m}) \right| \leq M \sum_{(-\infty \leq \bar{m} \leq \infty)} \sum \dots \sum |h(\bar{m})| < \infty. \quad (\text{A.2})$$

Thus the output sequence is bounded. The converse is proved by showing that if $S = \infty$, then a bounded input can be found that will cause an unbounded output. Such an input is the sequence:

$$x(\bar{m}) = \begin{cases} 1, & \text{if } h(-\bar{m}) \geq 0 \\ -1, & \text{if } h(-\bar{m}) \leq 0 \end{cases} \quad (\text{A.3})$$

From (A.1), the output at $(\bar{n}) = (\bar{0})$ is

$$y(0) = \sum_{(-\infty \leq \bar{m} \leq \infty)} \sum \dots \sum x(\bar{m})h(-\bar{m}) = \sum_{(-\infty \leq \bar{m} \leq \infty)} \sum \dots \sum |h(-\bar{m})|. \quad (\text{A.4})$$

which is equal to

$$y(0) = \sum_{(-\infty \leq \bar{m} \leq \infty)} \sum \dots \sum |h(\bar{m})| = S \quad (\text{A.5})$$

Therefore, if $S = \infty$, it follows that the output sequence is unbounded.

Appendix B

proof theorem 7

Assume $q_{\bar{\delta}}(z_0)$ is unstable, i.e. $q_{\bar{\delta}}(z_0) = 0$ and $|z_0| \leq 1$. If $Q(\bar{z})$ is stable, then

$$Q\left(z_0 \frac{\delta_1}{r}, z_0 \frac{\delta_2}{r}, \dots, z_0 \frac{\delta_N}{r}\right) = 0$$

where, $\left|z_0 \frac{\delta_i}{r}\right| > 1$ for some i , then $|z_0| > \left|\frac{r}{\delta_i}\right| > 1$ which is a contradiction.

If $Q(\bar{z})$ is unstable it follows that there is a $(\delta_1, \delta_2, \dots, \delta_N)$ where, $\max|\delta_i| \leq 1$ and $Q(\delta_1, \delta_2, \dots, \delta_N) = 0$.

If $q_{\bar{\delta}}(z)$ is stable, i.e.

$$q_{\bar{\delta}}(z) = Q\left(z \frac{\delta_1}{r}, z \frac{\delta_2}{r}, \dots, z \frac{\delta_N}{r}\right)$$

where, $r = \max|\delta_i|$.

then $q_{\bar{\delta}}(r) = 0$.

But, $r \leq 1$ which is a contradiction.

Proof of corollary 7

Assume as in the previous proof that $q_{\bar{\delta}}(z_0)$ is unstable, i.e. $q_{\bar{\delta}}(z_0) = 0$ for $|z_0| \leq 1$

If $Q(\bar{z})$ is stable, then

$$Q(z_0 \delta_1, z_0 \delta_2, \dots, z_0 \delta_N) = 0$$

where,

$|z_0 \delta_i| > 1$ for some i ,

or

$$|z_0| > \frac{1}{|\delta_i|} > 1$$

which is a contradiction.

If $Q(z)$ is unstable there exists a $(\delta_1, \delta_2, \dots, \delta_N)$ such that $\max|\delta_i| \leq 1$.

$$\text{Let } (\delta'_1, \delta'_2, \dots, \delta'_N) = \left(\frac{\delta_1}{r}, \frac{\delta_2}{r}, \dots, \frac{\delta_N}{r}\right)$$

where $r = \max|\delta_i|$.

Let

$$Q_{\bar{\delta}'}(z) = Q(z\delta'_1, z\delta'_2, \dots, z\delta'_N)$$

Then

$$Q_{\bar{\delta}'}(z) = Q(\delta_1, \delta_2, \dots, \delta_N) = 0$$

but $r \leq 1$ which is a contradiction.

Appendix C

Example of Minimal state-space realization of factorable 2-D transfer functions

C.0.1 problem statement

Consider the linear time invariant 2-D system, described by the spatial transfer function

$$H(z_1, z_2) = \frac{\sum_{i=0}^N \sum_{j=0}^M g_{i,j} z_1^{-i} z_2^{-j}}{\sum_{i=0}^N \sum_{j=0}^M h_{i,j} z_1^{-i} z_2^{-j}}, \quad (\text{C.1})$$

The problem considered in this paper is to determine a minimal state-space model of system (C.1) for the following two cases.

Case I:

The denominator coefficients of (C.1) can be arbitrary, while the numerator coefficients satisfy the following relationship:

$$g_{i,j} = g_{i,0} g_{0,j} \quad (\text{C.2})$$

where $g_{i,j}$ assumed, for simplicity, one

Case 2:

In the present case the numerator coefficients of (C.1) can be arbitrary, while the denominator coefficients satisfy the following relationship:

$$h_{i,j} = h_{i,0} h_{0,j} \quad (\text{C.3})$$

where $h_{i,j}$ assumed, for simplicity, one

The state-space model sought is of the Givone-Roesser type [1] described as follows:

$$\begin{bmatrix} x^h(n_1+1, n_2) \\ x^v(n_1, n_2+1) \end{bmatrix} = \begin{bmatrix} A_1 & A_2 \\ A_3 & A_4 \end{bmatrix} \begin{bmatrix} x^h(n_1, n_2) \\ x^v(n_1, n_2) \end{bmatrix} + \begin{bmatrix} B_1 \\ B_2 \end{bmatrix} u(n_1, n_2), \quad (\text{C.4})$$

$$y(n_1, n_2) = \begin{bmatrix} C_1 & C_2 \end{bmatrix} \begin{bmatrix} x^h(n_1, n_2) \\ x^v(n_1, n_2) \end{bmatrix} + Du(n_1, n_2), \quad (\text{C.5})$$

where $x^h(n_1, n_2) \in \mathbb{R}^{n_h}$ and $x^v(n_1, n_2) \in \mathbb{R}^{n_v}$, $u(i, j) \in \mathbb{R}_1$ is the input vector, and $y(i, j) \in \mathbb{R}_1$ is the output vector.

C.0.2 State-space realization

Case I

The spatial transfer function (C.1), when $g_{i,j} = g_{i,0}g_{0,j}$ (and $g_{0,0} = 1$), may be presented in a block diagram as in Fig. 1. A 2-D minimal state-space realization may be written by the inspection, from Fig. 1, having the form

(C.4) where

$$\begin{aligned}
 A_1 &= \begin{bmatrix} -\frac{h_{10}}{h_{00}} & 1 & 0 & \cdots & 0 \\ \cdot & 0 & \ddots & \ddots & \cdot \\ \vdots & \vdots & \ddots & \ddots & \vdots \\ \cdot & \cdot & \ddots & \ddots & 0 \\ \cdot & 0 & & \ddots & 1 \\ -\frac{h_{m0}}{h_{00}} & 0 & \cdot & \cdots & 0 \end{bmatrix}, \\
 A_2 &= \begin{bmatrix} \frac{h_{10}h_{01}}{h_{00}} - h_{11} & \cdots & \frac{h_{10}h_{0n}}{h_{00}} - h_{1n} \\ \vdots & \vdots & \vdots \\ \frac{h_{m0}h_{01}}{h_{00}} - h_{m1} & \cdots & \frac{h_{m0}h_{0n}}{h_{00}} - h_{mn} \end{bmatrix}, \\
 A_3 &= \begin{bmatrix} -\frac{1}{h_{00}} & 0 & \cdots & \cdots & 0 \\ 0 & 0 & \ddots & & \cdot \\ \vdots & \ddots & \ddots & \ddots & \vdots \\ \cdot & \cdot & \ddots & \ddots & 0 \\ \cdot & 0 & & \ddots & 0 \\ 0 & \cdots & \cdots & 0 & 0 \end{bmatrix}, \\
 A_4 &= \begin{bmatrix} -\frac{h_{01}}{h_{00}} & \cdots & \cdots & \cdot & \cdot & -\frac{h_{0n}}{h_{00}} \\ 1 & 0 & \cdots & \cdot & & 0 \\ 0 & \ddots & \ddots & & & \cdot \\ \vdots & \ddots & \ddots & \ddots & \ddots & \vdots \\ 0 & \cdots & \cdots & 0 & 1 & 0 \end{bmatrix},
 \end{aligned}$$

$$\begin{aligned} b_1 &= \begin{bmatrix} g_{10} - \frac{h_{10}}{h_{00}} \\ \vdots \\ g_{m0} - \frac{h_{m0}}{h_{00}} \end{bmatrix}, \\ b_2 &= \begin{bmatrix} \frac{1}{h_{00}} \\ \vdots \\ 0 \end{bmatrix}, \\ c_1 &= \begin{bmatrix} \frac{1}{h_{00}} & 0 & \cdots & 0 \end{bmatrix}, \\ c_2 &= \begin{bmatrix} g_{01} - \frac{h_{01}}{h_{00}} & \cdots & g_{0n} - \frac{h_{0n}}{h_{00}} \end{bmatrix}, \\ D &= \frac{1}{h_{00}}. \end{aligned}$$

Case 2

The 2-D transfer function (C.1), where $h_{ij} = h_{i0}h_{0j}$, may be presented in a block diagram form as in Fig. 3. A state-space realization may be written by

inspection from Fig. 3, using the Givone-Roesser form (C.4), where

$$A_1 = \begin{bmatrix} -h_{10} & . & \cdots & \cdots & . & -h_{1n} \\ 1 & 0 & \cdots & \cdots & \cdots & 0 \\ 0 & \ddots & \ddots & & & . \\ \vdots & \ddots & \ddots & \ddots & & \vdots \\ 0 & . & \cdots & 0 & 1 & 0 \end{bmatrix},$$

$$A_2 = \begin{bmatrix} 0 & \cdots & 0 \\ \vdots & & \vdots \\ 0 & \cdots & 0 \end{bmatrix},$$

$$A_3 = \begin{bmatrix} a_{11} & \cdots & a_{m1} \\ \vdots & & \vdots \\ a_{1n} & \cdots & a_{mn} \end{bmatrix},$$

$$A_4 = \begin{bmatrix} -h_{01} & 1 & 0 & \cdots & 0 \\ . & 0 & \ddots & \ddots & . \\ \vdots & \vdots & \ddots & & \vdots \\ . & . & & \ddots & 0 \\ . & . & & \ddots & 1 \\ -h_{0n} & 0 & . & \cdots & 0 \end{bmatrix},$$

$$b_1 = \begin{bmatrix} 1 \\ 0 \\ \vdots \\ 0 \end{bmatrix},$$

$$b_2 = \begin{bmatrix} g_{01} - h_{01}g_{00} \\ \vdots \\ g_{0n} - h_{0n}g_{00} \end{bmatrix},$$

$$c_1 = [g_{10} - h_{10}g_{00}, \cdots, g_{m0} - h_{m0}g_{00}],$$

$$c_2 = [1, 0, \cdots, 0],$$

$$D = g_{00}.$$

Appendix D

Proof that multi-variable polynomials cannot be factored in general

To establish that multi-variable polynomials cannot be factored in general, it is sufficient to show the insolvability of the problem in one particular case. If we assume $z_1^2 + z_2^2 + 1 = 0$ can be solved into a product of factors which are integral in z_1 and z_2 , i.e.,

$$\begin{aligned} z_1^2 + z_2^2 + 1 &= (pz_1 + qz_2 + r)(p'z_1 + q'z_2 + r') \\ &= pp'z_1^2 + qq'z_2^2 + rr' \\ &\quad + (pq' + p'q)z_1z_2 \\ &\quad + (pr' + p'r)z_1 \\ &\quad + (qr' + q'r)z_2 \end{aligned}$$

Since this is by hypothesis an identity, we can equate coefficients and obtain:

$$pp' = 1 \tag{D.1}$$

$$qq' = 1 \tag{D.2}$$

$$rr' = 1 \tag{D.3}$$

$$pq' + p'q = 0 \tag{D.4}$$

$$pr' + p'r = 0 \tag{D.5}$$

$$qr' + q'r = 0 \tag{D.6}$$

First we observe that, on account of equations (D.1), (D.2), and (D.3), none of the six quantities, p , q , r , p' , q' , r' can be zero and also $p' = \frac{1}{p}$, $q' = \frac{1}{q}$, $r' = \frac{1}{r}$. Thus, as a logical consequence of our hypothesis, we have, from (D.4), (D.5), and (D.6):

$$\frac{p}{q} + \frac{q}{p} = 0 \quad (\text{D.7})$$

$$\frac{p}{r} + \frac{r}{p} = 0 \quad (\text{D.8})$$

$$\frac{q}{r} + \frac{r}{q} = 0 \quad (\text{D.9})$$

and, from these again, if we multiply by pq , rp , and qr , respectively, we get

$$p^2 + q^2 = 0 \quad (\text{D.10})$$

$$p^2 + r^2 = 0 \quad (\text{D.11})$$

$$q^2 + r^2 = 0 \quad (\text{D.12})$$

Subtracting eq (D.12) from eq (D.11), we derive

$$p^2 - q^2 = 0 \quad (\text{D.13})$$

And from addition of eqs (D.10) and (D.13),

$$2p^2 = 0$$

From this it follows that $p = 0$, which is in contradiction with eq (D.1). Therefore, the solution in this case is impossible. q.e.d.